

Review

# Waste Biomass Selective and Sustainable Photooxidation to High-Added-Value Products: A Review

Liliana Llatance-Guevara <sup>1</sup>, Nelly Esther Flores <sup>2,\*</sup>, Germán Omar Barrionuevo <sup>3,4</sup>  and José Luis Mullo Casillas <sup>3,5</sup>

<sup>1</sup> Departamento de Ingeniería Química y Bioprocesos, Escuela de Ingeniería, Pontificia Universidad Católica de Chile, Avenida Vicuña Mackenna 4860, Macul, Santiago 8331150, Chile

<sup>2</sup> Research and Development Directorate, Faculty of Sciences, Food and Biotechnology, Technical University of Ambato, Ambato 180207, Ecuador

<sup>3</sup> Department of Mechanical and Metallurgical Engineering, School of Engineering, Pontificia Universidad Católica de Chile, Avenida Vicuña Mackenna 4860, Macul, Santiago 7820436, Chile

<sup>4</sup> Chemical and Materials Engineering Department, University of Alberta, Edmonton, AB T6G 1C9, Canada

<sup>5</sup> Facultad de Ciencias de la Ingeniería, Carrera de Ingeniería Mecánica, Universidad Técnica Estatal de Quevedo, Quevedo 120301, Ecuador

\* Correspondence: ne.flores@uta.edu.ec

**Abstract:** Researchers worldwide seek to develop convenient, green, and ecological production processes to synthesize chemical products with high added value. In this sense, lignocellulosic biomass photocatalysis is an excellent process for obtaining various outcomes for the industry. One issue of biomass transformation via heterogeneous catalysis into valuable chemicals is the selection of an adequate catalyst that ensures high conversion and selectivity at low costs. Titanium oxide (TiO<sub>2</sub>), is widely used for several applications, including photocatalytic biomass degradation, depolymerization, and transformation. Graphite carbon nitride (g-C<sub>3</sub>N<sub>4</sub>) is a metal-free polymeric semiconductor with high oxidation and temperature resistance and there is a recent interest in developing this catalyst. Both catalysts are amenable to industrial production, relatively easy to dope, and suited for solar light absorption. Recent investigations also show the advantages of using heterojunctions, for biomass derivatives production, due to their better solar spectrum absorption properties and, thus, higher efficiency, conversion, and selectivity over a broader spectrum. This work summarizes recent studies that maximize selectivity and conversion of biomass using photocatalysts based on TiO<sub>2</sub> and g-C<sub>3</sub>N<sub>4</sub> as supports, as well as the advantages of using metals, heterojunctions, and macromolecules in converting cellulose and lignin. The results presented show that heterogeneous photocatalysis is an interesting technology for obtaining several chemicals of industrial use, especially when using TiO<sub>2</sub> and g-C<sub>3</sub>N<sub>4</sub> doped with metals, heterojunctions, and macromolecules because these modified catalysts permit higher conversion and selectivity, milder reaction conditions, and reduced cost due to solar light utilization. In order to apply these technologies, it is essential to adopt government policies that promote the use of photocatalysts in the industry, in addition to encouraging active collaboration between photooxidation research groups and companies that process lignocellulosic biomass.

**Keywords:** biomass; lignocellulose; photocatalyst photooxidation; titanium dioxide (TiO<sub>2</sub>); carbon nitride (g-C<sub>3</sub>N<sub>4</sub>); noble-metals; heterojunctions; macromolecules; selective conversion



**Citation:** Llatance-Guevara, L.; Flores, N.E.; Barrionuevo, G.O.; Mullo Casillas, J.L. Waste Biomass Selective and Sustainable Photooxidation to High-Added-Value Products: A Review. *Catalysts* **2022**, *12*, 1091. <https://doi.org/10.3390/catal12101091>

Academic Editors: Detlef W. Bahnemann, Ewa Kowalska, Ioannis Konstantinou, Magdalena Janus, Vincenzo Vaiano, Wonyong Choi and Zhi Jiang

Received: 18 August 2022

Accepted: 13 September 2022

Published: 21 September 2022

**Publisher's Note:** MDPI stays neutral with regard to jurisdictional claims in published maps and institutional affiliations.



**Copyright:** © 2022 by the authors. Licensee MDPI, Basel, Switzerland. This article is an open access article distributed under the terms and conditions of the Creative Commons Attribution (CC BY) license (<https://creativecommons.org/licenses/by/4.0/>).

## 1. Introduction

Biomass is a plentiful and carbon-neutral renewable energy source that may be used to create platform chemicals and fuels, especially considering that up to 75% of initial energy can be converted into biofuels. Lignocellulosic biomass comprises lignin, cellulose, and hemicellulose; lignin is almost 30% of the organic carbon in the biosphere. However, this lignin is regarded as waste material in several industries, for example, during paper TA and agricultural production, leaving significant amounts of biomass that contaminates the

planet [1]. By 2035, bioenergy could provide 10% of the world's primary energy, according to the International Energy Agency (IEA), and biofuels may potentially replace up to 27% of global transportation fuel by 2050 [2]. According to Granone et al. [2] around 100 billion tons of biomass are produced worldwide each year, which makes it an available resource for obtaining biofuels [3] and chemical products with high added value [4–6].

Hydrocarbon compounds obtained from biomass have been used as intermediate molecules to produce chemical compounds and fuels. Biomass components (cellulose and lignin) have significant applications in the manufacture of various bio-based materials for solar energy, energy conversion, and storage devices [7–11]; it is especially true about lignin, and lignin derivatives. However, lignocellulose is more challenging to transform than municipal and other industrial organic wastes. Biomass's advantage is not being edible, avoiding the depletion of food sources to obtain commodity chemicals or fuels [12]. Lignocellulose is very recalcitrant; thus, it is necessary to break down this component into little fractions to facilitate its conversion into valuable products, such as sugars, alcohols, phenols, furan derivatives, levulinic acid and  $\gamma$ -valerolactone, gluconic acid, 2,5-Furandicarboxylic acid, and more [13–16] or direct use as lignin nanoparticles that are useful for biomedical applications [17]. Some processes applied to lignocellulose transformation are gasification, pyrolysis [18], and hydrolysis, which all require high pressure and temperature fragmentation steps. Besides, the conversion and selectivity percentages reached are low, which a challenge to making this process profitable with a high yield in conversion and selectivity of degradation reactions [19]. The conservation of resources and high energy cost necessitate testing new processes requiring milder reaction conditions, such as biochemical and catalytic methods [20,21]. Heterogeneous photocatalysis emerges as a clean and very selective technology to obtain specific products from biomass. Titanium dioxide is the star catalyst used for biomass transformation because it is widely available, inexpensive, nontoxic, chemically, and physiologically inert, and stable when exposed to solar light. However, it has a band gap of 3.2 eV and can only absorb in the U.V. light spectrum, decreasing solar light energy conversion efficiency [22]. Titanium dioxide can produce several components under varying reaction conditions, making this catalyst a base for developing new modified catalysts [22,23]. To address the apparent disadvantages of titanium dioxide, several studies have investigated how to increase the TiO<sub>2</sub> performance during the conversion of biomass derivatives into additional products by doping it with different metals or macromolecules [24–26], and even using this catalyst as the base for developing new heterojunctions [27,28]. Studies have replaced TiO<sub>2</sub> by other catalysts, such as graphite g-C<sub>3</sub>N<sub>4</sub>, to improve selectivity and conversion [29–34] and they are also interesting to review in order to have more options to transform biomass into useful products.

For these reasons, the photocatalytic process for the selective conversion of biomass derivatives is visualized as a sustainable and innovative technology because it is simple and low-cost. Moreover, the solar energy used in the process is abundant. It is one of the most economical alternative energy resources, which is transformed into chemical energy with the help of photocatalysts [35–37]. In this sense, photocatalysis of biomass reduces fossil fuel consumption, which minimizes environmental problems [38,39].

During the last decade, the number of investigations on obtaining chemical products from biomass has increased. However, it is necessary to identify what type of catalysts provide higher conversion and selectivity. Understanding which materials facilitate photooxidation is essential to promote the use of photocatalysts that facilitate the conversion of biomass to products of interest to the industry. Therefore, this literature review provides a new perspective regarding the selective conversion of lignocellulosic biomass to contribute to future studies of heterogeneous photocatalysis, and inspire the development of new and better photocatalysts with highly efficient properties, and thus be able to obtain high conversion percentages and selectivity. As a hypothesis, it is proposed to determine if doping TiO<sub>2</sub> and g-C<sub>3</sub>N<sub>4</sub>, with noble metals helps to generate greater conversion and selectivity in the photocatalytic reaction of biomass derivatives towards chemical products

with high added value, as well as to determine if the addition of  $\beta$ -cyclodextrin on the surface of photocatalysts will shorten the reaction time in the conversion.

This review is organized as follows. The methodology adopted to classify the most pertinent articles is presented in Section 2. Then, the main concepts related to biomass and its derivatives are detailed in Section 3. Section 4 recounts a summary of the mechanisms involved in heterogeneous photocatalysis. Then, the most used photocatalysts are presented in Section 5, highlighting titanium dioxide ( $\text{TiO}_2$ ), carbon nitride ( $\text{g-C}_3\text{N}_4$ ), noble metals, and the applicability of heterojunctions and macromolecules. Then the conversion of cellulose and lignin is presented in Section 6, and finally, the main conclusions and perspectives for future work are set out.

## 2. Materials and Methods

The methodology employed to carry out this review centers on the keywords: “photocatalysis,” “biomass,” and “chemical products” using the Boolean operator AND, resulting in a total of 91 documents indexed in the Web of Science database (Figure 1). The last search was performed on 15 May 2022. Since 2016, it is possible to notice how the interest in obtaining chemical products from biomass has grown. Thus, in 2020 the number of publications doubled compared to 2018 and 2019, and the trend continues. Figure 2 shows relevant papers about the photocatalytic transformation of biomass, where the studies of Colmenares et al. [5] and Lang et al. [40] stand out. It is worth noting that Figure 2 arranges papers according to their similarity but is not a citation tree. Related reports show connecting lines and clusters. The larger the bubble, the more citations; the darker colors indicate recently published papers.

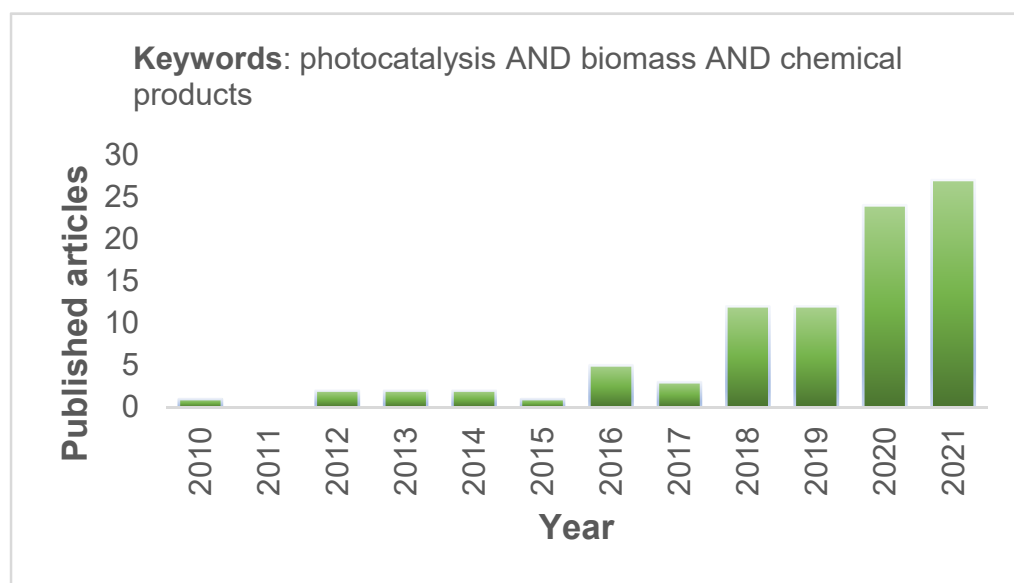


**Figure 1.** Published articles in the last decade focused on photocatalysis, biomass, and chemical products reported in the Web of Science database.

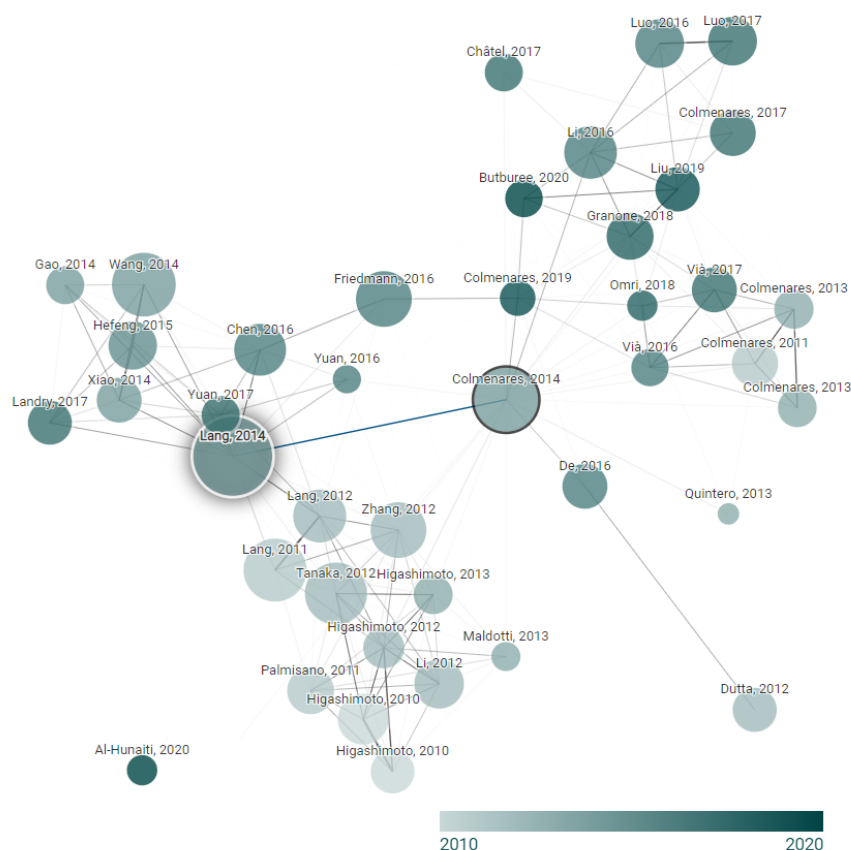


**Figure 2.** Relevant papers on the field of photocatalysis and biomass in the last decade taken from connected papers.

### 3. Biomass

Lignocellulosic biomass is the primary structural component of plant matter and is mostly inedible, generally referring to organic materials such as wood, grass, and agricultural crop residues [41,42]. The principal lignocellulosic biomass components are: lignin (20–30% *w/w*), cellulose (35–50% *w/w*) and hemicellulose (20–30% *w/w*) [41,42]. Regarding the structure of lignocellulosic biomass (Figure 3), the external cell of the biomass, which provides rigidity to the material, is rich in lignin [43,44]. It is a macromolecular polyaromatic with a high oxygen content [45,46]. On the other hand, cellulose is found inside lignin and forms hemicellulose-bound shells with a random structure. It is a stable crystalline biopolymer made of glycoside units. These units are insoluble in most solvents and difficult to hydrolyze [47]. Hemicellulose has an amorphous structure of pentose sugars such as xylose and arabinose, and hexose carbohydrates such as glucose, mannose, and galactose, so it is easier to hydrolyze than cellulose [10,47].

Although processing complex lignocellulosic materials is one of the main obstacles to commercial-scale biofuels and renewable chemicals, stimulating biofuel production has economic, environmental, and societal benefits. Different types of photocatalysts and reactors have been studied to decompose and process lignocellulosic biomass (or its components) [48,49].

Bio-oil is obtained from the lignocellulosic biomass conversion through thermal, catalytic, or both processes combined. The resulting bio-oil comprises oxygenated monomers such as cresols and guaiacols [6,50]. However, due to its high oxygen content, bio-oil is unstable and has a low energy content, and requires additional treatment to be used industrially [51]. Consequently, the transformation of platform molecules from lignocellulosic biomass (starting materials or building blocks to produce chemical products) has been identified as critical in converting biomass into fuels and chemical compounds [52]. The goal is to replace petrochemical compounds with renewable and sustainable com-

pounds progressively. Moreover, the derivatization of compounds from biomass is crucial in recovering chemical products.

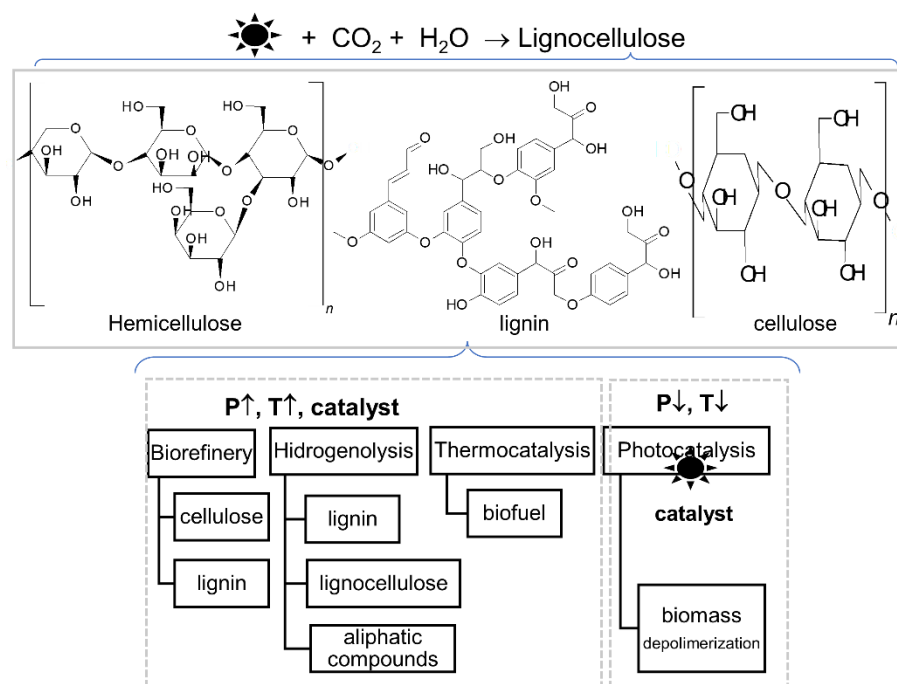


**Figure 3.** Routes for the recovery of lignocellulosic biomass [10]. Adapted with permission from Nature/Springer/Palgrave, *Nature Catalysis*, Solar energy-driven lignin-first approach to full utilization of lignocellulosic biomass under mild conditions, Xuejiao W. et al., License Number: 5382740520618, 2018.

Some of the factors responsible for the attractiveness of biomass as a renewable source for conversion to chemical products are climate change and reduction in greenhouse gases [53], the need to search for renewable carbon sources as an alternative to fossil sources [53], the possibility to optimize the process of obtaining energy and chemical products [54], and finally, increasing public trust in the chemical business.

Selective oxidation of derivatives of lignocellulosic biomass is a promising process for obtaining chemical products in a sustainable way [55]. The biggest challenge is to make this process profitable with a high conversion yield and selectivity of degradation reactions. However, producing these chemicals requires high temperatures and high pressures, which results in increased energy consumption [56]. Furthermore, the conversion and selectivity percentages are low [44,45,57]. For this reason, the photocatalytic process for the selective conversion of biomass derivatives is viewed as a sustainable and innovative technology. Because it is simple and low-cost, solar energy used in the process is abundant and is one of the cheapest alternative energy resources; photocatalytically, this can be transformed into chemical energy.

#### 4. Heterogeneous Photocatalysis

In recent years, heterogeneous photocatalysis has been regarded as one of the most promising technologies for addressing environmental issues and the global energy crisis [57–59]. This process is one of the cleanest because it needs few reactants, operates under smooth conditions, and takes advantage of visible and ultraviolet (U.V.) light [59–63]. Heterogeneous photocatalysis is a mechanism of absorbing direct or indirect radiant radiation (visible or U.V.) using a broadband semiconductor. It is feasible to activate it when the catalyst absorbs a photon with an energy equal to or greater than the bandgap ( $B_g$ ); for example, solar radiation promotes electron transport from the valence band (V.B.) to the

conduction band (C.B.) [64]. In this way, hole-electron pairs ( $h^+e^-$ ) are formed, which are charge carriers for photochemical oxidation and reduction reactions (Equation (1)) [63–68].



Some of the pollutants that have been degraded by heterogeneous photocatalysis are rhodamine B [69], amoxicillin [70], tetracycline antibiotics [71], tetracycline hydrochloride [72], and phenol [73]. Based on these works, it is possible to state that the approach is effective because the deterioration percentages in all the experiments exceeded 70%. Moreover, in recent years this process has also been implemented to obtain specific chemical products, such as the selective photo-reduction of carbon dioxide ( $\text{CO}_2$ ) to hydrocarbons [61,62,74,75]. Some clear examples are the studies developed by Ahmed et al. [76] and Tasbihi et al. [77], where methane is obtained. Selective photooxidation has also been used to produce aldehydes from alcohols [59,78]. López-Tenllado et al. [79] studied the oxidation of 2-butenol (crotyl alcohol) to 2-butenal (crotonaldehyde), achieving 70% conversion and 90% selectivity after 90 min of reaction. It was also shown that these processes are substantially influenced by the reaction time and pH of the solution. In addition, there are various intermediates between the reagents and the end products, which provide convenient control over the selective reactions of certain bonds in the lignin derivatives to obtain useful chemical products [65,80]. Another advantage of the photocatalytic process is that the reactions can be carried out at mild conditions, such as room temperature and atmospheric pressure, thanks to a photon interchange instead of thermal energy [81]. Thus, it is possible to promote the selective photooxidation of by-products of lignocellulosic biomass. It is possible to obtain the so-called platform molecules that include a great variety of carboxylic acids [42,53,82].

Success in the photocatalysis process lies in the proper use of photocatalysts since they are the ones that use solar energy to promote the transport of electrons from the V.B. to the C.B. as seen in Figure 4 [7,65,83]. In heterogeneous photocatalysis, one electron ( $e^-$ ) jumps up from the valence band to the conduction band, after absorbing a photon with higher energy than the bandgap energy. This leap leaves a vacancy called a hole ( $h^+$ ) in the V.B. [84]. Electrons carry out the reduction process in the conduction band. The most typical reduction method is biomass photo-reforming, which involves the reduction of a proton by an  $e^-$  to form hydrogen ( $\text{H}_2$ ). During this process, photoinduced holes oxidize lignocellulose or its derivatives, lowering the recombination rate of photogenerated hole-electron pairs and boosting the water-splitting efficiency [85].

It is possible to obtain value-added products when intermediate partially oxidized products are determined as the final product. Photocatalytic holes produce oxidative radicals that directly or indirectly oxidize specific organic molecules [86]. An oxidative hole, for example, reacts with hydroxyl ions ( $\text{OH}^-$ ) to form hydroxyl radicals ( $\bullet\text{OH}$ , potential redox: +2.81 V versus standard hydrogen electrode (SHE)) [1,8,40,86]. Then, the oxidative radicals target the biomass molecules; for example, Figure 5 shows a lignin photo-reforming process, where reactive  $\bullet\text{OH}$  radicals degrade lignin due to the bond cleavage of  $\beta\text{-O-4}$  [87]. This lignin bond break results in the generation of benzyl, alkoxy, and alkyl radicals that produce lignin fragments with a low molecular weight during the depolymerization reaction. Hydroxyl and  $\bullet\text{OH}$  radicals can also directly attack lignin's phenyl rings forming catechol, resorcinol, and hydroquinone [88]. During the photocatalytic process, other reactive oxygen species can be formed, including superoxide anions ( $\text{O}_2^{\bullet-}$ , potential redox: +0.89 V versus SHE), singlet molecular oxygen ( $\text{O}_2$ ), and ozone  $\text{O}_3$  [62,63].

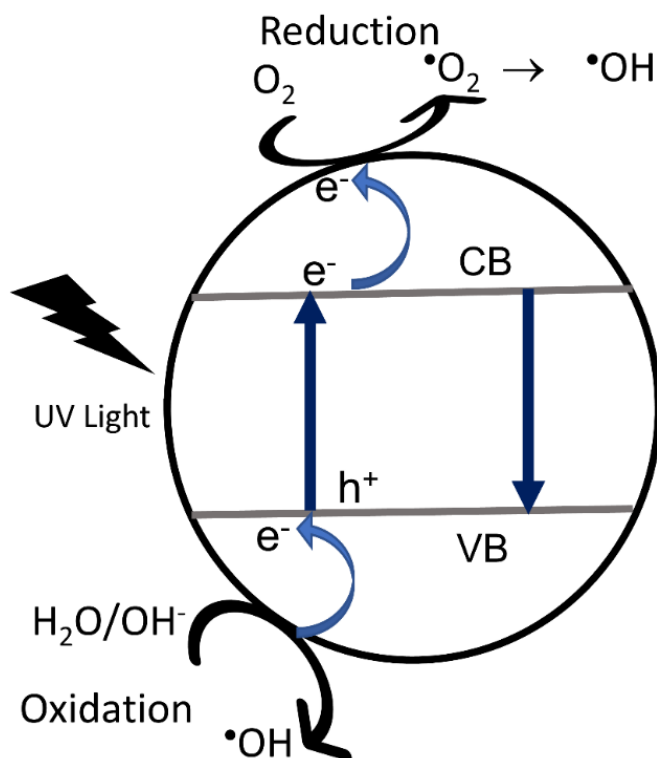


Figure 4. Mechanism of heterogeneous photocatalysis [64].

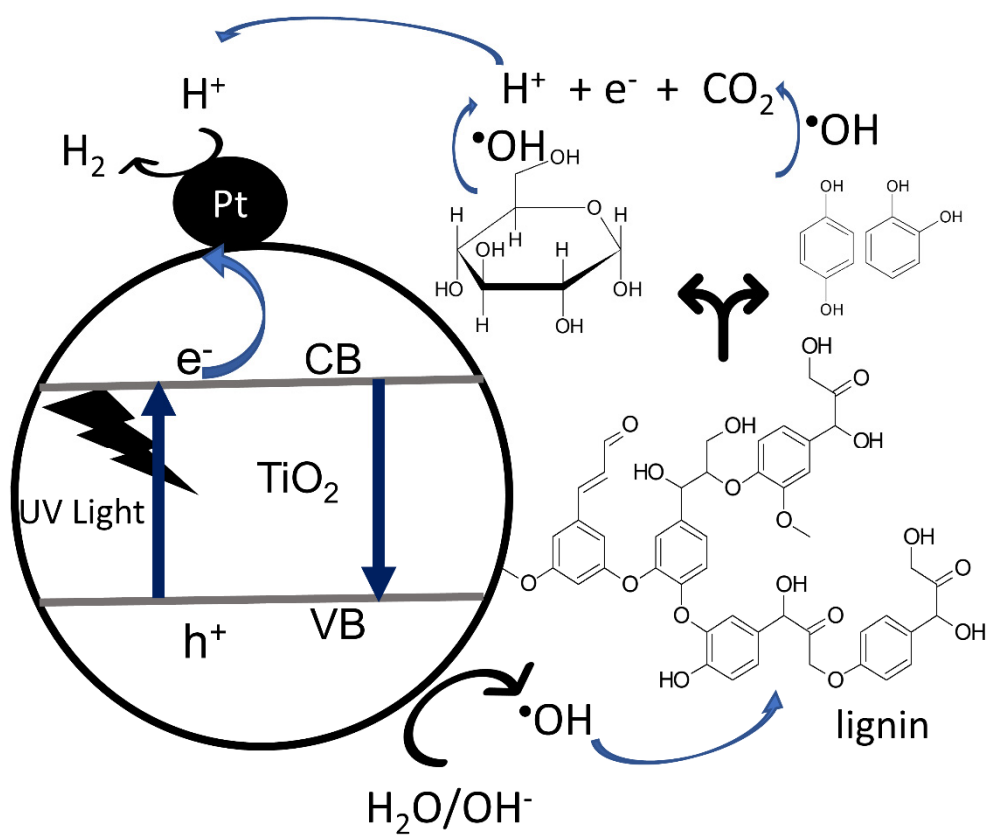


Figure 5. Lignin photo-reforming process directly attacks lignin's phenyl rings, forming catechol and hydroquinone [87].

## 5. Photocatalysts for Biomass Conversion

The photocatalyst nature is the central part of the heterogeneous photocatalysis process. The success in biomass degradation and conversion reactions depends on its properties [58,89]. One of the most remarkable properties of  $\text{TiO}_2$  is absorbing visible light, which permits it to work at an industrial level with sunlight [90,91]. Several works have been identified in which  $\text{TiO}_2$  and  $g\text{-C}_3\text{N}_4$  have been used as successful photocatalysts for different degradation processes and some selective conversions, such as selective oxidation of alcohols to aldehyde [58,91]. In several studies, combining photocatalysts with other metals provided them with new and better properties. This doping increases the conversion and selectivity while improving the reaction yields [59,71,92]. The following section presents the major advances in photocatalysts, highlighting doping with noble metals, heterojunctions, and macromolecules to improve the performance of photocatalysts based on titanium dioxide and carbon nitride.

### 5.1. Titanium Dioxide $\text{TiO}_2$

Titanium dioxide ( $\text{TiO}_2$ ) is one of the most used and attractive heterogeneous photocatalysts, especially in processes of degradation of pollutants in [73,93], due to its excellent properties such as high photocatalytic activity, strong oxidizing capacity, chemical stability, long durability, non-toxicity, low cost, and transparency to visible light [94]. The difficulty is that it has a bandgap in the ultraviolet area of the electromagnetic spectrum with an energy of 3.23 eV [70,94], i.e.,  $\text{TiO}_2$  can only use between 3% and 5% of the solar spectrum of visible light, in addition to the recombination of excited pairs ( $h^+e^-$ ), which restricts its applications in photocatalysis [91–99]. There are several crystalline structures of  $\text{TiO}_2$ , e.g., anatase, rutile, and brookite titanium dioxide; they differ in their three-dimensional form, as can be seen in Figure 6.

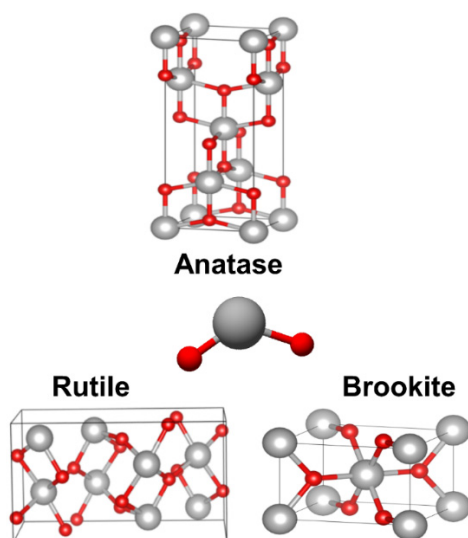


**Figure 6.** Anatase (tetragonal), rutile (tetragonal), and brookite (orthorhombic), structures of  $\text{TiO}_2$  [100–102]. This figure was created using VESTA Version 3, with permission from Journal of Applied Crystallography, VESTA 3 for three-dimensional visualization of crystal, volumetric and morphology data, K. Momma and F. Izumi, Free Software, 2011.

In 1996, it was suggested that anatase's conduction band is 0.2 eV higher than that of rutile because the flat band potential of anatase is 0.2 eV lower than that of rutile, as seen in Figure 7; at an interface, this promotes photogenerated electron transfer from anatase to rutile and hole transfer from rutile to anatase [103,104]. However, new photoemission experiments show that the work function of anatase is 0.2 eV higher than that of rutile, implying that anatase's conduction band is 0.2 eV lower than that of rutile, and thus implying more light absorption [105,106].

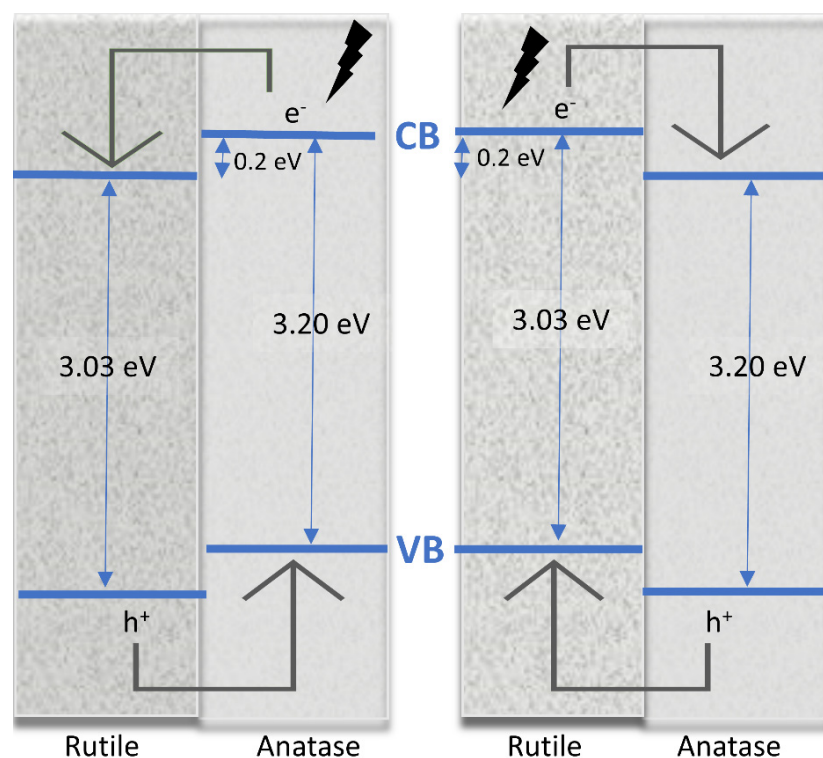


**Figure 7.** Two valence and conduction band alignment processes for the anatase/rutile interaction. The image on the left presents the transfer of photogenerated electrons from anatase to rutile, and the image on the right displays the recent photoemission measurements from rutile to anatase. Adapted with permission from Nature/Springer/Palgrave, *Nature Materials*, Band alignment of rutile and anatase TiO<sub>2</sub>, Scanlon D.O. et al., License Number: 5391770708077, 2013 [106].

### 5.2. Carbon Nitride (*g*-C<sub>3</sub>N<sub>4</sub>)

Carbon nitride (*g*-C<sub>3</sub>N<sub>4</sub>) has a stable structure and semiconductor characteristics [93,107]. It has a bandgap energy of approximately 2.88 eV, allowing greater visible light absorption than TiO<sub>2</sub> [107,108]. It has an excellent photocatalytic performance, strong chemical stability, and good resistance to acid and alkali corrosion, making it a favorite in photocatalysis. Furthermore, it is easy to synthesize since it only requires a calcination step of readily available precursors such as cyanamide, melamine, or urea (in the range of 500–580 °C for 1–4 h) [109,110]. However, some defects have also been reported, such as a small specific area, low separation degree of electrons and holes, and a limited visible light range for some reactions [109,111].

The search for photocatalysts with higher efficiency in separating photogenerated pairs has become an important research field. Photocatalytic systems related to carbon nitride are practical and efficient for the spatial separation of photogenerated electron-hole pairs; furthermore, they permit the development of heterostructures based on *g*-C<sub>3</sub>N<sub>4</sub> [90,110,112]. The heterostructures based on *g*-C<sub>3</sub>N<sub>4</sub> offer superior photocatalyst qualities due to the synergy between *g*-C<sub>3</sub>N<sub>4</sub> and the other components of the heterostructures. The heterostructures based on *g*-C<sub>3</sub>N<sub>4</sub> may inhibit the recombination of photogenerated charge carriers offering better photocatalyst qualities [90,113].

The construction of photocatalysts with high efficiency driven by visible light for environmental and energy applications, as well as lowering processing time, may be possible by the design of *g*-C<sub>3</sub>N<sub>4</sub>-based heterostructures; Figure 8 [71,90,113].

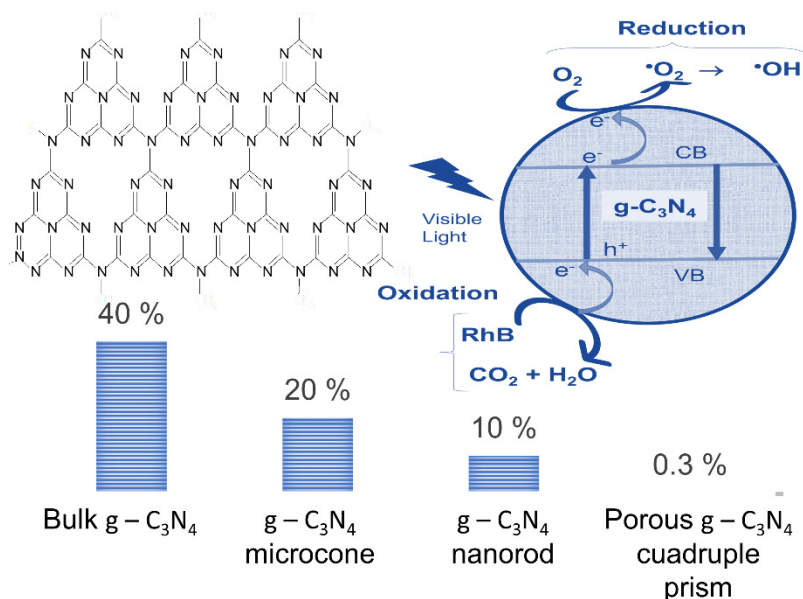


**Figure 8.** Photocatalytic activity of  $g\text{-C}_3\text{N}_4$  under visible light with five different morphologies after 120 min of treatment [90]. Adapted with permission from Elsevier, *Materials Science in Semiconductor Processing*, Effect of morphology on the photocatalytic activity of  $g\text{-C}_3\text{N}_4$  photocatalysts under visible-light irradiation, Xingtong W. et al., License Number: 5391770315356, 2015.

### 5.3. Doping with Noble Metals

Catalyst doping involves the addition of a foreign species to the catalytic system; therefore, the original activity of the catalyst varies. To improve the efficiency of sun-driven photocatalysis, noble metal nanoparticles (N.P.s) extend the U.V. absorption characteristics of  $\text{TiO}_2$  and  $g\text{-C}_3\text{N}_4$  to the visible area [111,114]. Surfaces doped with noble metals such as Au, Ag, Pd, and Pt lead to enhanced photogenerated electron transfer and lifetime extension of carriers'. As a result of localized surface plasmon resonance, N.P.s can absorb visible light and hence activate broadband semiconductors (e.g.,  $\text{TiO}_2$ ) on the visible light spectrum [96,110,112,114].

In the study of Darabdhara et al. [114], the degradation of several phenolic compounds by photocatalysis was analyzed, and an oxidation process was observed.

Table 1 summarizes the primary metals used in the photocatalysis process, while Table 2 details the obtained reagents and products and conversion and selectivity percentages.

**Table 1.** Bandgap of the component-doped catalysts [96,97,115,116].

| Catalyst                 | Metal | Bandgap (eV) |
|--------------------------|-------|--------------|
| $g\text{-C}_3\text{N}_4$ | -     | 2.88         |
|                          | Ag    | 2.86         |
|                          | Pt    | 2.7          |
|                          | Pd    | 2.78         |
|                          | Au    | 2.79         |
| $\text{TiO}_2$           | -     | 3.23         |
|                          | Ag    | 3.17         |
|                          | Pt    | 3.08         |
|                          | Pd    | 3.05         |
|                          | Au    | 3.1          |

**Table 2.** Examples of selective conversion using catalysts with bimetallic doping at  $\lambda$  ( $\lambda > 400$  nm).

| Photocatalyst                              | Reactive        | Product         | % Conversion | % Selectivity | Ref.  |
|--|-----------------|-----------------|--------------|---------------|-------|
| g-C <sub>3</sub> N <sub>4</sub>            | Benzyl          |                 | 5.7          |               |       |
| Ag/g-C <sub>3</sub> N <sub>4</sub> (1%)    | alcohol         |                 | 12.3         |               |       |
| Pd/g-C <sub>3</sub> N <sub>4</sub> (1%)    |                 | Imine           | 31.7         | >99           | [111] |
| Ag-Pd/g-C <sub>3</sub> N <sub>4</sub> (1%) |                 |                 | 31.4         |               |       |
| Ag-Pd/g-C <sub>3</sub> N <sub>4</sub> (2%) |                 |                 | 58.9         |               |       |
| TiO <sub>2</sub>                           |                 |                 |              | 42.11         |       |
| Pt/TiO <sub>2</sub>                        | CO <sub>2</sub> | CH <sub>4</sub> | 50           | 74.21         | [96]  |
| Ag/TiO <sub>2</sub>                        |                 |                 |              | 84.52         |       |
| Pt-Ag/TiO <sub>2</sub>                     |                 |                 |              | 87.9          |       |

The intermediate products were catechol, hydroquinone, and p-benzoquinone; the photocatalyst used was g-C<sub>3</sub>N<sub>4</sub>. It was possible to prove that when g-C<sub>3</sub>N<sub>4</sub> was doped with metallic N.P.s, the photocatalytic process presented a 90% percentage of degradation, compared to the 42% obtained when using no modified photocatalyst. Furthermore, it was shown that the process was more efficient when working with sunlight than with U.V. light, so it is concluded that the use of noble metals favors the absorption of light in the visible spectrum [109,117].

#### 5.4. Heterojunctions

Another technique used to achieve high efficiency in space charge separation and extend light absorption to the visible range is the construction of heterojunctions, which involve the combination of two or more semiconductors depending on their band gaps [89,118].

Straddling, staggered and broken gap heterojunctions are based on the alignment of energy levels, as shown in Figure 9. The first type indicates that the bandgap of the semiconductor-I is wider than that of semiconductor-II, the V.B. of the semiconductor-I is below that of the semiconductor-II, and the C.B. of the semiconductor-II is higher than the C.B. of the semiconductor-I, forming a space that can take both directions. Due to this, the migration of charge carriers generates an accumulation of electrons and holes that occurs only in the semiconductor-I, which causes poor charge separation of the photogenerated pairs of electrons and holes, in addition to a lower redox potential because the oxidation and reduction reactions occur in the same semiconductor [64]. In the second heterojunction type, the band positions are at optimal levels (staggered gap), offering a space charge carrier for enhanced photocatalytic separation compared to type I. However, its redox potential is low due to oxidation and reduction reactions that occur in semiconductor-I with lower oxidation potential and semiconductor-II with lower reduction potential [89,118,119]. Type III heterojunctions have a broken gap involving charge carrier separation, similar to type II heterojunctions [42–62,119]. The broken bandgap of the heterojunction in type III does not cross and does not cause charge carrier separation to enhance photocatalytic activity.

In this way, the Z scheme is formed and the electrons receiving the irradiation of visible light in the C.B. of semiconductor-II are combined with holes of the photogenerated V.B. of semiconductor-I. This combination leads to the formation of sufficiently strong oxidative V.B. holes in semiconductor-II and reducing electrons in the C.B. of semiconductor-I, as seen in Figures 9 and 10. Due to the band difference, the induced interface results in an electric field capable of accelerating the separation of the photogenerated pairs ( $h^+e^-$ ) [118,119].

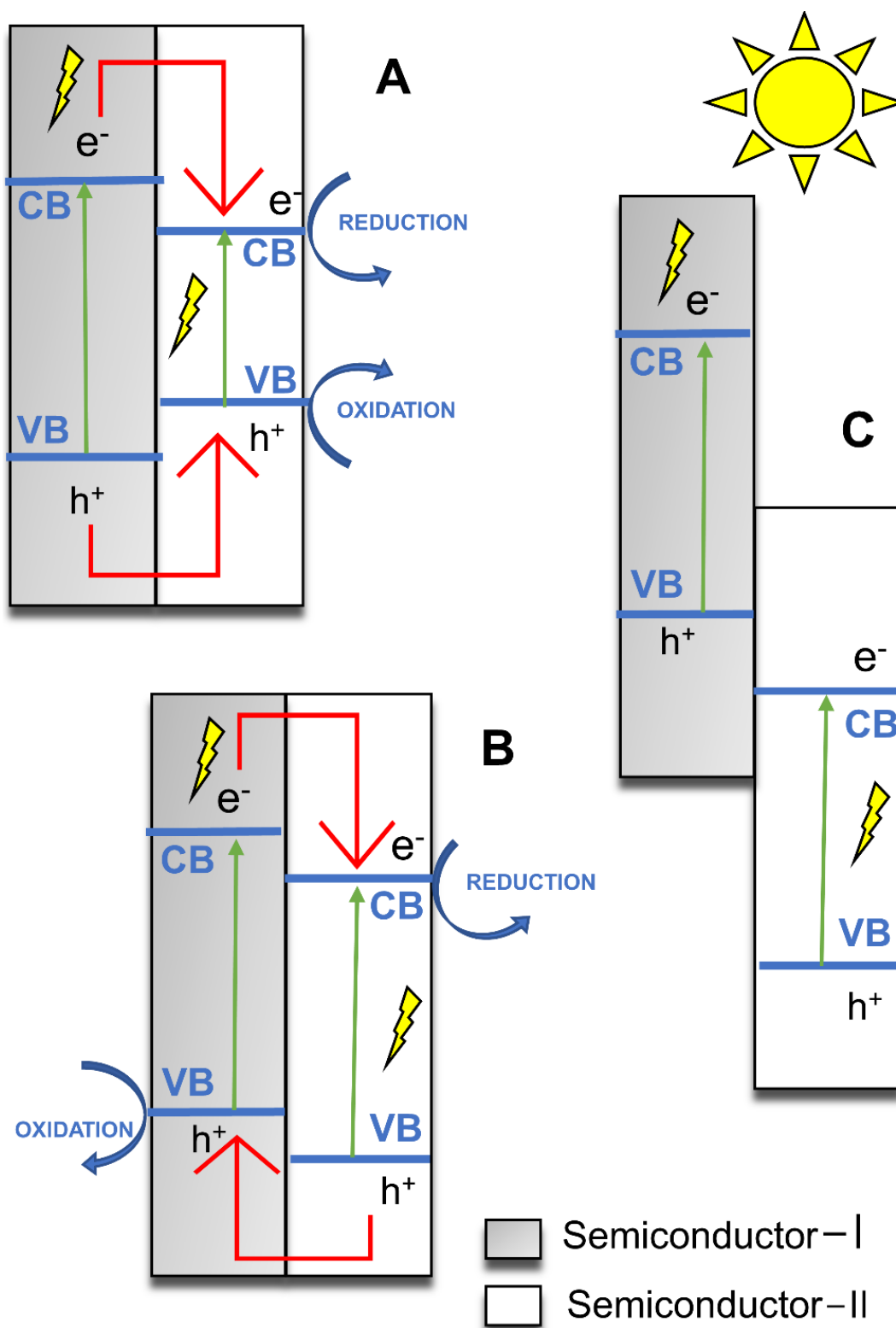


**Figure 9.** Progression of the Z scheme in photocatalysis, including (A) type I, straddling gap, (B) type II, staggered gap, and (C) type III, broken gap [89]. Adapted with permission from Wiley-VCH Verlag GmbH & CO. KGAA, *Advanced Materials*, Heterojunction Photocatalysis, Low J. et al., License Number: 1270478-1, 2017.

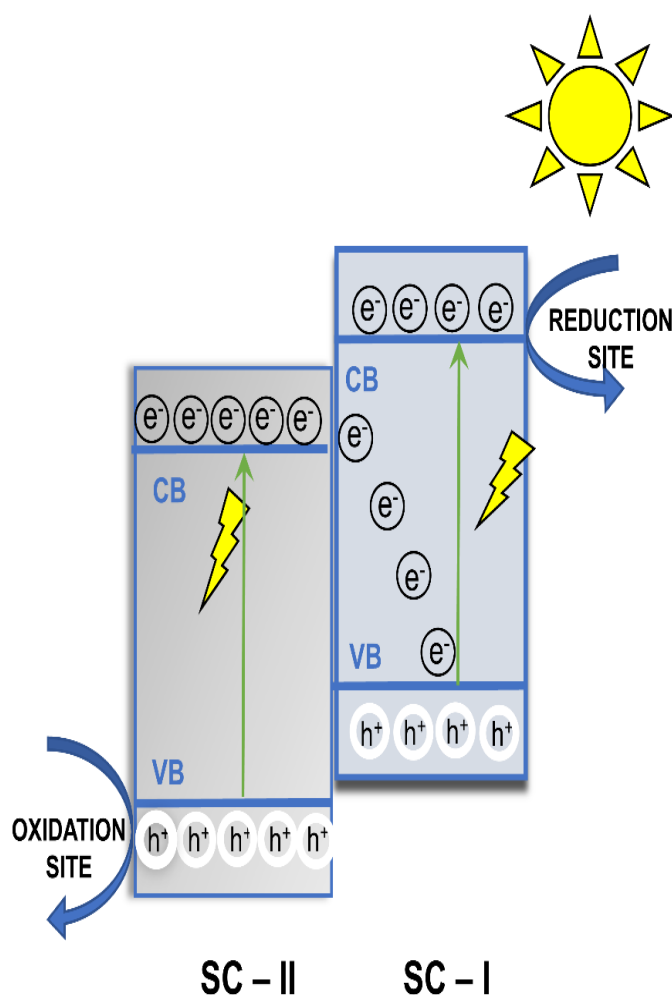


**Figure 10.** Z-Scheme of [119] Adapted with permission from Elsevier, *Journal of Industrial and Engineering Chemistry*, An overview of converting reductive photocatalyst into all solid-state and direct Z-scheme system for water splitting and CO<sub>2</sub> reduction, Raizada P. et al., License Number: 5391800879853, 2021.

The scheme name, Z, Figure 11, is proposed because it mimics photosynthesis in plants and follows the same charge transfer pathway mechanism containing two-step photoexcitation, which shows resemblance to the letter “Z” [89,119].

Some studies show that converting biomass-derived molecules into other more valuable ones is possible using middle reaction conditions. For example, Shao et al. [120] developed the Co/ZnO@C heterojunction catalyst for biomass derivative hydrogenation that permitted the selective hydrogenation of levulinic acid to  $\gamma$ -valerolactone, achieving 89.28% conversion and 92.47% selectivity at 120 °C, 2 MPa, and 4 h reaction conditions, improving previous investigations that needed higher temperature and pressure [6,121] Moreover, Chen et al. [121] converted furfural into cyclopentanone using their catalyst fabricated of a Ni–NiO heterojunction supported on TiO<sub>2</sub> with anatase and rutile (Ni–NiO/TiO<sub>2</sub>-Re450), achieving 100% conversion and 84.7% yield under 1 MPa, 140 °C, and 6 h reaction conditions. Both examples show that heterojunctions improve the performance of commonly used catalyzers such as TiO<sub>2</sub>, lowering the reaction conditions and reducing energy costs if they are going to be applied at the industrial scale [122].

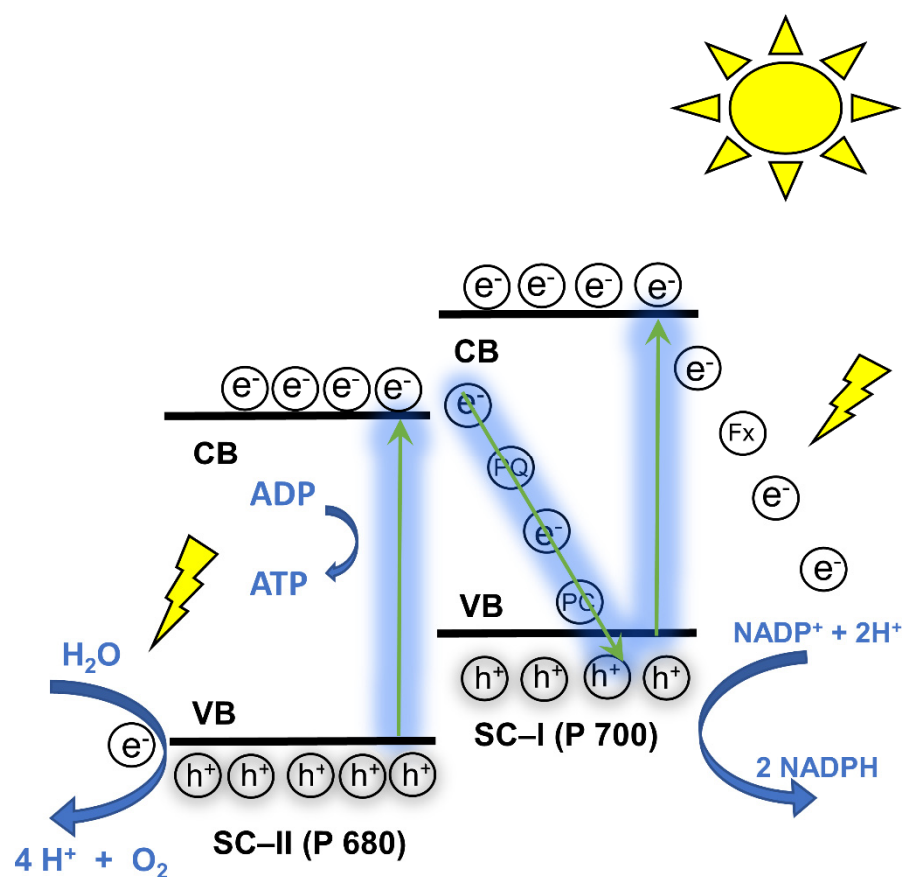


**Figure 11.** Natural photosynthesis mimicking the Z scheme [119]. Adapted with permission from Elsevier, *Journal of Industrial and Engineering Chemistry*, An overview of converting reductive photocatalyst into all solid-state and direct Z-scheme system for water splitting and CO<sub>2</sub> reduction, Raizada P. et al., License Number: 5391800879853, 2021.

### 5.5. Photocatalysts Modified by Macromolecules

It is possible to modify photocatalysts, adding macromolecules on the surface, e.g., cyclodextrins (C.D.s), which are biodegradable cyclic hydrocarbons [123].  $\beta$ -Cyclodextrin ( $\beta$ -CD) is essential in photogenerated charge transfer, as it can serve as a hole eliminator to suppress recombination of photogenerated ( $h^+e^-$ ) pairs. It has also been shown that its presence contributes to a more selective reaction because it prevents the formation of the  $\bullet$ OH radical, which is highly reactive but not selective, so its presence contributes to complete degradation reactions, obtaining as final products CO<sub>2</sub> and H<sub>2</sub>O [95,124].

Cyclodextrins (C.D.s) commonly contain 6, 7, or 8 units of  $\alpha$ -D-glucose and are called  $\alpha$ ,  $\beta$ , and  $\gamma$ -cyclodextrins, respectively [123,125]. C.D.s have a well-defined conical structure, Figure 12, with the broad rim surrounded by the secondary  $-OH$  groups and the narrow rim surrounded by the primary  $-OH$  groups [123,125]. The cyclodextrin has two faces: a hydrophobic inner and a hydrophilic outer; these characteristics allow C.D.s to form macromolecular complexes with a wide variety of organic and inorganic compounds that result in changes in the essential features of the compounds associated with them [63,126].

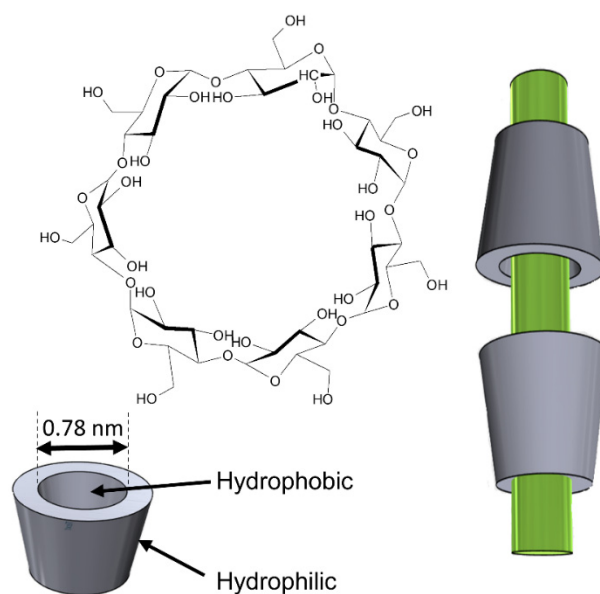


**Figure 12.** The chemical structure and form of  $\beta$ -cyclodextrin [127].

Chen et al. [128] evaluated the degradation of naphthalene under visible light; they concluded that Ag-NPs added to the photocatalyst improved the absorbance in the visible region. On the other hand, the photocatalyst activity that contains  $\beta$ -CD traps the naphthalene inside it because its cavity is hydrophobic. Thus, the naphthalene molecules remain in contact with the surface photocatalyst for a longer time, which favors a more efficient reaction. Finally, experiments under visible light, with the photocatalyst containing Ag-NPs and  $\beta$ -CD, presented the highest photocatalytic activity, reaching a degradation of 98.4% of naphthalene in 150 min, as shown in Figure 13. This work demonstrates the possibility of modifying photocatalysts to make them efficient and work with visible light, which can be used since it is known that the combination between metals and  $\beta$ -CD provides new and better properties to the photocatalyst [128]. Therefore, it could be taken to an industrial application since only sunlight is required to activate the photocatalysts.

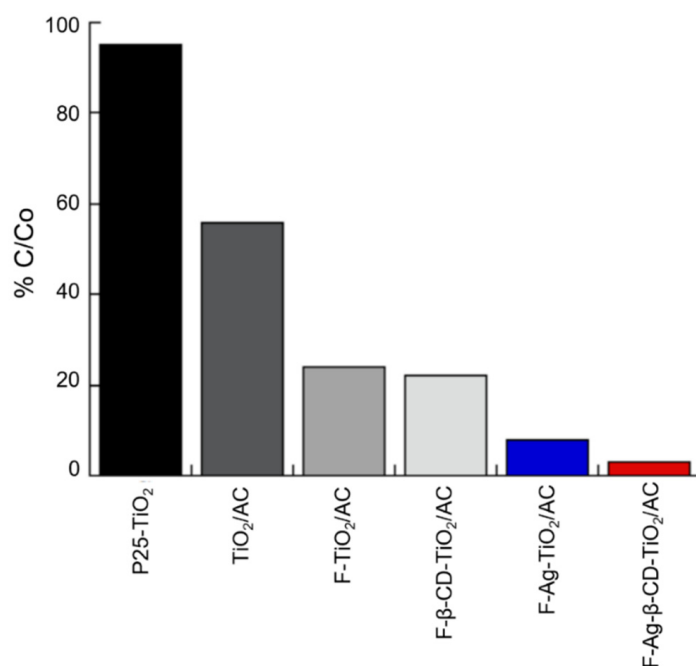


**Figure 13.** Photocatalytic degradation rate of naphthalene on seven different photocatalysts irradiated with visible light after 150 min of treatment [128].

## 6. Lignocellulosic Biomass Conversion Using Photocatalysts

### 6.1. Cellulose Conversion

Cellulose is a D-glucose linear polymer linked by b-1,4 glycosidic bonds; it is the most abundant biomass component in nature [2,86,129]. In addition to understanding the biomass photodegradation pathway, it is essential to design and manufacture suitable photocatalysts with excellent properties such as easy mass diffusion, light-harvesting, and improved separation of photogenerated pairs to obtain high conversion percentages and selectivity [6,59,71,92,129]. In selective photooxidation processes of compounds derived from cellulose, high-value chemical products have been obtained among the so-called platform molecules that include a wide variety of carboxylic acids such as succinic, fumaric, and malic acids, 2,5-furandicarboxylic, 3-hydroxy propionic, aspartic, glucaric, glutamic, itaconic, and levulinic acids, and other basic molecules (3-hydroxybutyrolactone, glycerol, sorbitol and xylitol/arabitol) [6,22,86,130].

Colmenares and Magdziarz [42] studied the photocatalytic oxidation of glucose, where three organic compounds were obtained as a result: glucaric acid (GUA), gluconic acid (G.A.), and arabitol (AOH). These carboxylic acids are fundamental building blocks in manufacturing pharmaceuticals, foods, perfumes, and fuels [9,131]. Figure 14 summarizes the results obtained for glucose conversion and selectivity for GUA and G.A. using different photocatalysts immersed in three water-acetonitrile mixes (10% H<sub>2</sub>O/90% ACN, 50% H<sub>2</sub>O/50% ACN, 100% H<sub>2</sub>O). As can be observed, working with TiO<sub>2</sub> (U.S.) results in higher selectivity (total selectivity for GUA + GA is 71.3%) with 11.0% glucose conversion. In this work for all TiO<sub>2</sub> photocatalysts, the selectivity depends on the acetonitrile content in the mixture, although the relationship is not proportional; for example, using 50% ACN selectivity is better than 90% ACN mixtures.

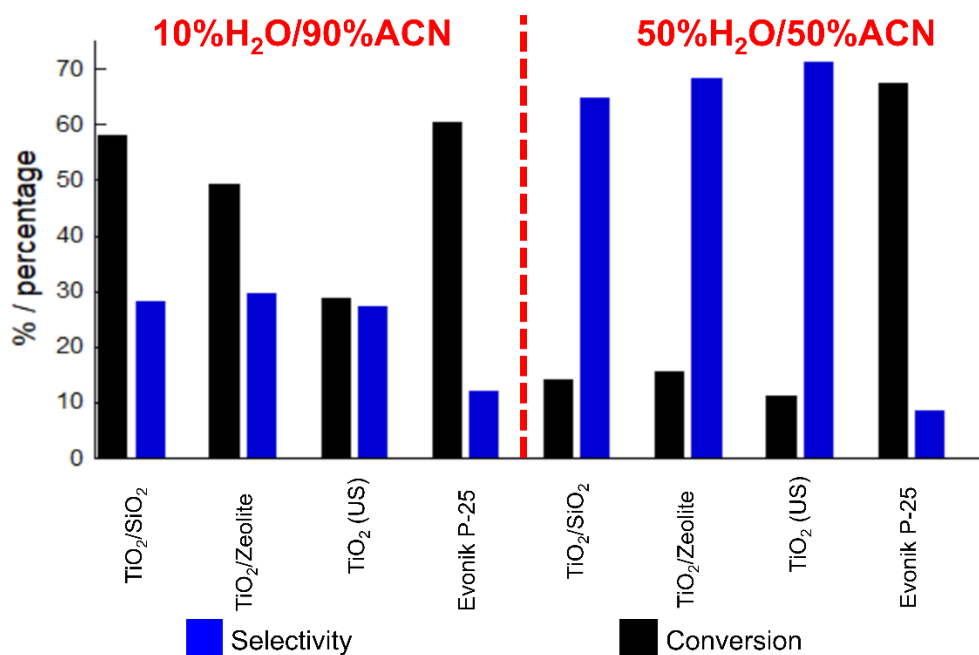


**Figure 14.** Effect of solvent composition on the conversion and selectivity of glucose to carboxylic acids using different TiO<sub>2</sub> photocatalysts, under 2.8 mM of glucose concentration, 150 mL of solution, 150 mg of photocatalyst, 30 °C, 1 bar, and 10 min illumination time [42].

Another example of conversion of cellulose derivatives is reported by Jin et al. [132], where formic acid is obtained as a product of glucose conversion. This process is mainly attributed to the acceleration in the development of active oxidative radicals (O<sub>2</sub><sup>•−</sup>, •OH) in the presence of hydroxyl ions. Furthermore, hydroxyl ions regulate the charge of the TiO<sub>2</sub> surface and glucose adsorption and formic acid desorption, resulting in conversion of 79.6% and selectivity of 14.2%.

Payormhorm et al. [9], proposed a mechanism of conversion of glucose to gluconic acid, arabinose, xylitol, and formic acid, as shown in Figure 15. Three significant reactions are required to convert glucose into these compounds. First, a nucleophilic attraction of H<sub>2</sub>O molecules initiates these •OH radicals on the TiO<sub>2</sub> surface at O lattice sites (Ti-O•). When these H<sub>2</sub>O molecules come into contact with holes in the valence band of TiO<sub>2</sub>, they are oxidized to •OH. These •OH radicals oxidize glucose into gluconic acid. By photocatalytic decarboxylation, the gluconic acid transforms into arabinose and formic acid. Another possible reaction pathway is the photocatalytic decomposition of glucose to produce xylitol. The efficiency of the photodegradation process depends on the amount of energy that is radiated in the process; one exciting route is the conversion of glucose to gluconic acid and xylitol because, in this process, the energy consumption was reduced, and it was carried out under mild conditions compared to thermochemical catalysts and biological processes [9,133].

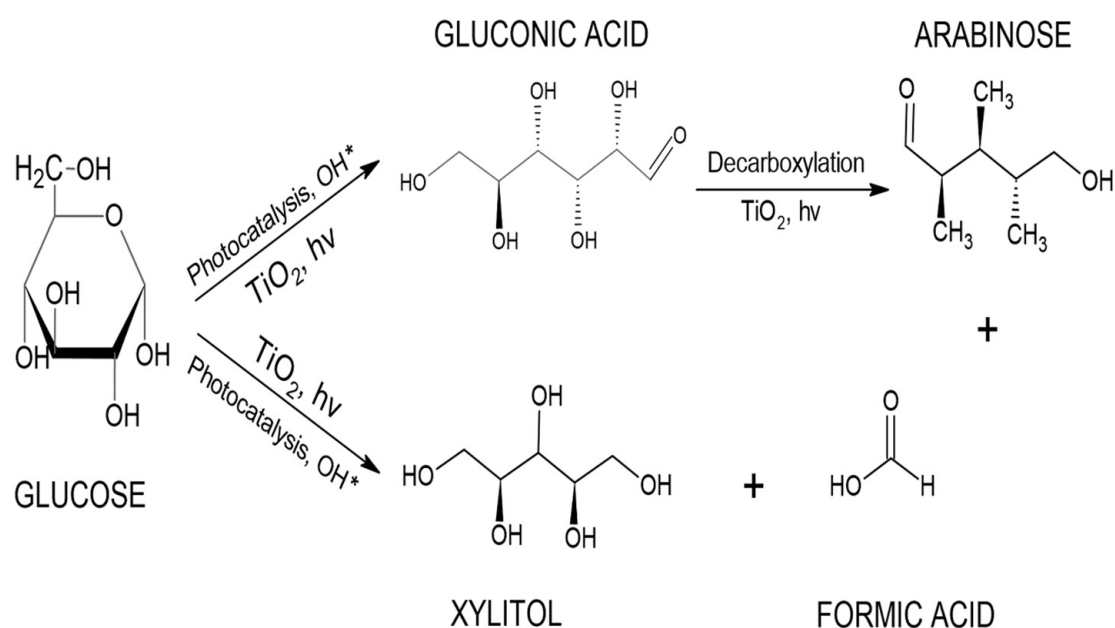


**Figure 15.** Reaction pathways proposed for the TiO<sub>2</sub> photocatalytic conversion of glucose into gluconic acid, arabinose, xylitol, and formic acid [9].

These findings pave the way for developing a novel strategy process and the economically viable usage of sustainable biomass and clean solar energy to manufacture formic acid. It is interesting that sugars such as glucose, fructose, xylose, mannose, and arabinose can be extracted from biomass, but chemical processes combined with photooxidation are still needed to achieve good recoveries and high selectivity [134]. Figure 16 depicts the results obtained in the work of Bellardita et al. [22,135], where TiO<sub>2</sub> was used as a photocatalyst in its three phases, anatase, rutile, and brookite. Each was modified with metallic doping of Pt and compared under ultraviolet light for a selective glucose conversion reaction to produce arabinose, erythrose, fructose, gluconic acid, glucaric acid, formic-acid, H<sub>2</sub>, and CO<sub>2</sub>. This study revealed that the distribution depends on the structural and physicochemical characteristics of the photocatalyst. Therefore, it is possible to obtain the desired product by controlling the process. For example, to obtain gluconic acid, it is observed that the only photocatalyst that provides this product is Pt-anatase. Similarly, Pt-rutile helps produce in large proportion formic acid as a final product.

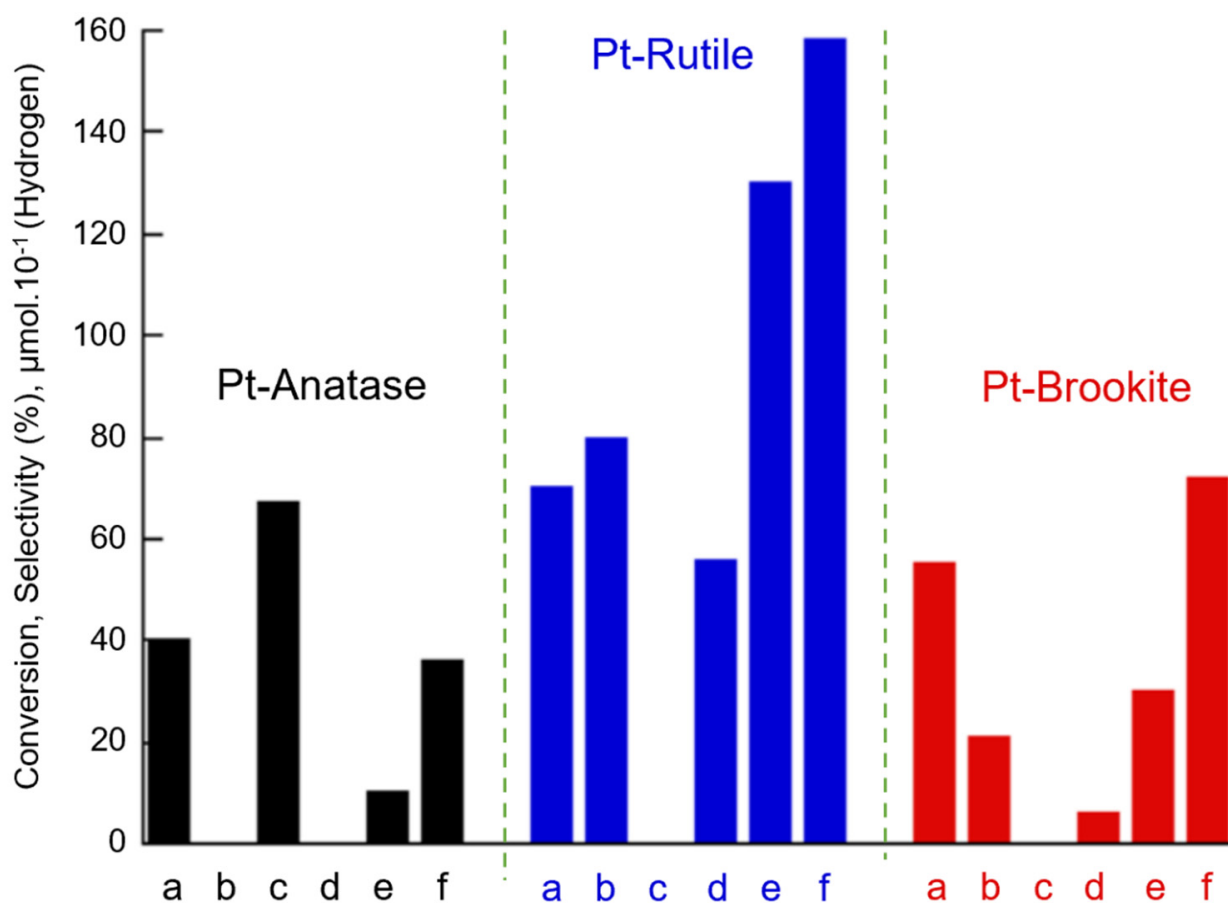


**Figure 16.** (a) Glucose conversion; (b) selectivity of arabinose, (c) selectivity of gluconic acid, (d) selectivity of erythrose, (e) selectivity of formic acid, and (f) amount of hydrogen obtained during the transformation in the presence of Pt-TiO<sub>2</sub> samples (anatase, rutile, brookite) [21,135]. Adapted with permission from Bentham Science Publishers Ltd., *Mini-reviews in organic chemistry*, Bellardita, M. et al., License Number: 1270489-1, 2020.

Table 3 indicates the main products reported in the literature, the operating conditions, and the photocatalyst for cellulose and glucose conversion. It is evident that the products obtained after the conversion depend on the photocatalyst and the type of light used during the process. Therefore, there a wide field of research is necessary to obtain specific compounds with high conversion percentages.

**Table 3.** The photocatalytic conversion of cellulose and its derivatives using four different catalysts.

| Substrate | Photocatalyst             | Light                 | Conversion (%) | Products  | Ref.  |
|-----------|---------------------------|-----------------------|----------------|---|-------|
| Glucose   | TiO <sub>2</sub>          | Mercury lamp (400 W)  | 6.45           | Xylitol<br>Gluconic acid                        | [9]   |
| Cellulose | CdS/CdOx                  | Simulated solar light | 9.7            | H <sub>2</sub>                                  | [85]  |
| Cellulose | Au-HYT                    | Visible light         | 59             | Glucose<br>HMF                                  | [136] |
| Cellulose | Pt-TiO <sub>2</sub> (P25) | U.V.                  | 66             | Arabinose<br>Erythrose<br>HMF<br>H <sub>2</sub> | [137] |

## 6.2. Lignin Conversion

The depolymerization of oxygen-enriched lignin is facilitated primarily by selective cleavage of C-O bonds, in aryl ethers by cleavage of C-O-C bonds, and further hydrogenol-

ysis of phenolic dimers to deoxygenated biofuels [138]. However, lignin's complex and irregular structure often misleads the search for selective chemical conversion; other known depolymerization approaches often produce vague and indistinct products in less quantity [138,139]. In this sense, photocatalysis is a promising and advantageous approach to replace or unify different techniques to induce selective oxidation of lignocellulosic biomass. It is a low molecular mass feedstock source through pretreatment; it further processes lignin model compounds into other value-added fine chemicals [140].

The specific photocatalytic conversion of poorly structured lignin into valuable chemicals is directly related to its strong oxidizing power for selective chemical transformations [141]. It is currently known that different strategies have been studied to update and improve the effectiveness of the photocatalytic conversion of lignin, which include, among others, the design of heterostructures through a combination of semiconductors with other hybrid materials, e.g., heteroatom doping (or compound formation) and heterojunctions, by combining the semiconductors with secondary semiconductors, noble metals, and carbon-based materials [89,141].

The major products of lignin oxidative breakdown are aromatic aldehydes and carboxylic acids. In the oxidative deconstruction of lignin, vanillin is a standard product, with yields ranging from 5 to 15% *w/w* concerning the lignin source [40]. Vanillin is a valuable industrial chemical used as a flavoring agent in food, cosmetics, pharmaceutical, nutraceutical, and fine chemical industries [134,141].

After the lignin degradation process, it is possible to identify different molecules as the final product: acetic acid, malonic acid, succinic acid, butylated hydroxytoluene, vanillin, veratric acid, and palmitic acid [132,141]. Catechol, resorcinol, and hydroquinone are first produced during the photodegradation of phenolic compounds employing  $\text{TiO}_2$  as a photocatalyst. The phenyl rings in these compounds are broken to yield malonic acid and short-chain organic acids, such as maleic, oxalic, acetic, and formic acids, until the sample is mineralized, at which point  $\text{CO}_2$  is produced as the ultimate product of the degradation process [60,94].

Figure 17 shows the results obtained by Kamwilaisak et al. [140]; here, a graphic representation of the percentages of identified intermediate compounds of lignin is observed for each experiment. All treated lignin samples had a comparable amount of fatty acids, 15%, while in the standard lignin samples, the percentage was only 10%. Carbohydrate was detected in the highest concentration in the biocatalytic reaction sample (20%), whereas it was insignificant in the photocatalytic reaction. In mono- and two-step reaction samples, the carbohydrate content was 10% and 5%, respectively. The highest organic acid concentration was measured in the photoreaction process, reaching 20%. This effect could be attributed because the photoreaction can produce compounds such as short-chain organic acids before finally degrading or fully mineralizing to  $\text{CO}_2$  [42,142]. Some of these synthesized acids are of commercial interest, e.g., succinic, acetic, and lactic acids.

Table 4 shows that  $\text{TiO}_2$ —and modified  $\text{TiO}_2$ —are the main photocatalysts used to convert lignin into useful industrial products such as vanillin. It is necessary to choose the right type of lignin and the suitable  $\text{TiO}_2$ -modified catalyst to obtain specific products. Data in Table 4 also indicate that more than 40.3% of biomass converts during the photooxidation process—avoiding polluting residues—and more research is necessary in cases where the conversion is low.

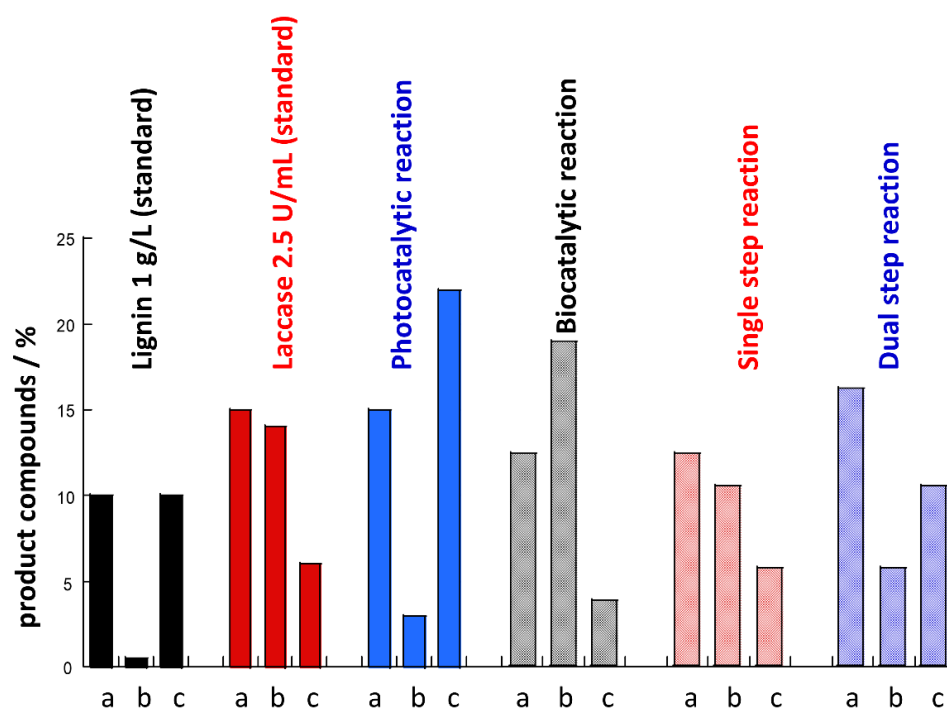


**Figure 17.** The percentage of intermediate compounds from lignin—(a) fatty acids, (b) carbohydrates, and (c) organic acids—from experiments conducted in the absence of H<sub>2</sub>O [140] Adapted with permission from American Chemical Society, *Energy & Fuels*, Kamwilaisak, K., Wright, P.C., Copyright 2012.

**Table 4.** Summary of results of the photocatalytic conversion of lignin and its derivatives.

| Substrate      | Photocatalyst   | Light Source                    | Conversion (%) | Main Products                                 | Ref.  |
|----------------|---|---------------------------------|----------------|---|-------|
| Lignosulfonate | Bi1%/Pt15-TiO <sub>2</sub>  | Xe lamp (300 W)                 | 84.5           | Guaiacol                                      | [91]  |
| Lignin         | TiO <sub>2</sub> Lacasse<br>H <sub>2</sub> O <sub>2</sub>             | UV irradiation (24 W)           | 100            | Organic acids<br>Fatty acids<br>Carbohydrates | [140] |
| Kraft lignin   | TiO <sub>2</sub> /carbon  | Mercury lamp (400 W)            | 40.3           | Vanillin                                      | [143] |
| Kraft lignin   | TiO <sub>2</sub> /Ti/Ta <sub>2</sub> O <sub>5</sub> -IrO <sub>2</sub> | Blue wave TM 50 AS UV spot lamp | 92             | Vanillin<br>Vanillic acid                     | [144] |

## 7. Perspectives and Conclusions

Through this bibliographic review, we seek to provide a direction that will facilitate the development of future works based on the heterogeneous photocatalysis process, since efficient methods are needed to convert waste biomass into chemical products with high added value. Although the results presented here are encouraging, it is necessary to evaluate the photooxidation process not only at a laboratory scale, but also at an industrial level.

For the process to be profitable at an industrial level, it must be carried out with sunlight, and it is necessary to repeat experiments at pilot scale and not only at the laboratory level. For this reason, the importance of working with photocatalysts that are capable of absorbing visible light is highlighted. As a result, it will be essential to conduct an economic study to evaluate whether the process is lucrative and if it necessary to modify

the photocatalysts so that they can absorb visible light. In addition, it should be considered that most of the studies are carried out with derivatives of lignocellulosic biomass or bio-oil, so it is necessary to study the direct photocatalytic degradation of biomass.

The heterogeneous photocatalysis process is presented as a viable technique for converting renewable energies such as lignocellulosic biomass and solar energy into fuels and chemicals. In this review, several works of interest are summarized in terms of their achievements in percentages of photocatalytic conversion of lignocellulosic biomass and its derivatives. The importance of breaking the bonds was identified thanks to the oxidizing power of the photocatalysis process to obtain chemical products with high added value, taking into account that the process must be controlled to prevent biomass derivatives from fully mineralizing to CO<sub>2</sub> and H<sub>2</sub>O.

Titanium dioxide is the most useful catalyst employed to convert biomass into new valuable products; this study showed several experiences where its catalytic ability increased when TiO<sub>2</sub> was doped with a proper metal or macromolecule. In the case of g-C<sub>3</sub>N<sub>4</sub>, the dopage with noble metals helped increase the biomass's selective conversion. Furthermore, the modified catalyzers decreased the temperature, pressure, and time during reactions, reducing energy and cost. The obtained products depend highly on the catalyst used, while the reaction conditions affect the conversion and selectivity. The addition of β-cyclodextrin on the surface of photocatalysts contributes to complete degradation reactions, decreasing the conversion time. It is crucial to note that further investigation will permit the design of customized catalysts for specific purposes.

The review lets us realize that it is possible to design custom catalysts, from TiO<sub>2</sub>, and g-C<sub>3</sub>N<sub>4</sub>, to obtain specific products from biomass with the minimum time and energy consumption.

A problem that became apparent during the investigation is that at the end of the photocatalytic process, separating and purifying the products obtained from the reaction medium represent a significant challenge. The study of separation methods is required to obtain products with high added value.

For this technology to be implemented at an industrial level, it is imperative to plan public policies that integrate advances in academia with industry needs, and thus define a roadmap for obtaining greater participation of bioenergy and biofuels and reduce dependence on non-renewable sources.

**Author Contributions:** Conceptualization: L.L.-G., supervision: G.O.B. and N.E.F., literature search: L.L.-G. and G.O.B., material preparation: L.L.-G., J.L.M.C., methodology: G.O.B. and N.E.F., acquisition of data: L.L.-G., interpretation of data: N.E.F., J.L.M.C., writing—original draft: L.L.-G., writing—review and final editing: G.O.B. and N.E.F. All authors have read and agreed to the published version of the manuscript.

**Funding:** This work was funded by ANID Chile DOCTORADO NACIONAL/2020-21211313 and the Research and Development Directorate, Technical University of Ambato.

**Data Availability Statement:** Not applicable.

**Acknowledgments:** The authors gratefully acknowledge funding from ANID Chile DOCTORADO NACIONAL/2020-21211313, SENESCYT grant No. ARSEQ-BEC-000329-2017, Research and Development Directorate, Technical University of Ambato.

**Conflicts of Interest:** The authors declare no competing interests.

## References

1. Li, S.H.; Liu, S.; Colmenares, J.C.; Xu, Y.J. A Sustainable Approach for Lignin Valorization by Heterogeneous Photocatalysis. *Green Chem.* **2016**, *18*, 594–607. [[CrossRef](#)]
2. Granone, L.I.; Sieland, F.; Zheng, N.; Dillert, R.; Bahnemann, D.W. Photocatalytic Conversion of Biomass into Valuable Products: A Meaningful Approach? *Green Chem.* **2018**, *20*, 1169–1192. [[CrossRef](#)]
3. Gallezot, P. Conversion of Biomass to Selected Chemical Products. *Chem. Soc. Rev.* **2012**, *41*, 1538–1558. [[CrossRef](#)]
4. Sheldon, R.A. Green and Sustainable Manufacture of Chemicals from Biomass: State of the Art. *Green Chem.* **2014**, *16*, 950–963. [[CrossRef](#)]

5. Colmenares, J.C.; Luque, R. Heterogeneous Photocatalytic Nanomaterials: Prospects and Challenges in Selective Transformations of Biomass-Derived Compounds. *Chem. Soc. Rev.* **2014**, *43*, 765–778. [[CrossRef](#)]
6. Jing, Y.; Guo, Y.; Xia, Q.; Liu, X.; Wang, Y. Catalytic Production of Value-Added Chemicals and Liquid Fuels from Lignocellulosic Biomass. *Chem* **2019**, *5*, 2520–2546. [[CrossRef](#)]
7. Lan, J.; Lin, J.; Chen, Z.; Yin, G. Transformation of 5-Hydroxymethylfurfural (HMF) to Maleic Anhydride by Aerobic Oxidation with Heteropolyacid Catalysts. *ACS Catal.* **2015**, *5*, 2035–2041. [[CrossRef](#)]
8. Clarizia, L.; Apuzzo, J.; Di Somma, I.; Marotta, R.; Andrezzi, R. Selective Photo-Oxidation of Ethanol to Acetaldehyde and Acetic Acid in Water in Presence of TiO<sub>2</sub> and Cupric Ions under U.V.-Simulated Solar Radiation. *Chem. Eng. J.* **2019**, *361*, 1524–1534. [[CrossRef](#)]
9. Payormhorm, J.; Chuangchote, S.; Kiatkittipong, K.; Chiarakorn, S.; Laosiripojana, N. Xylitol and Gluconic Acid Productions via Photocatalytic-Glucose Conversion Using TiO<sub>2</sub> Fabricated by Surfactant-Assisted Techniques: Effects of Structural and Textural Properties. *Mater. Chem. Phys.* **2017**, *196*, 29–36. [[CrossRef](#)]
10. Wu, X.; Fan, X.; Xie, S.; Lin, J.; Cheng, J.; Zhang, Q.; Chen, L.; Wang, Y. Solar Energy-Driven Lignin-First Approach to Full Utilization of Lignocellulosic Biomass under Mild Conditions. *Nat. Catal.* **2018**, *1*, 772–780. [[CrossRef](#)]
11. Liu, X.; Duan, X.; Wei, W.; Wang, S.; Ni, B.J. Photocatalytic Conversion of Lignocellulosic Biomass to Valuable Products. *Green Chem.* **2019**, *21*, 4266–4289. [[CrossRef](#)]
12. Singhvi, M.S.; Gokhale, D.V. Lignocellulosic Biomass: Hurdles and Challenges in Its Valorization. *Appl. Microbiol. Biotechnol.* **2019**, *103*, 9305–9320. [[CrossRef](#)]
13. Scott, E.; Peter, F.; Sanders, J. Biomass in the Manufacture of Industrial Products—the Use of Proteins and Amino Acids. *Appl. Microbiol. Biotechnol.* **2007**, *75*, 751–762. [[CrossRef](#)]
14. Girisuta, B.; Heeres, H.J. Levulinic Acid from Biomass: Synthesis and Applications. In *Production of Platform Chemicals from Sustainable Resources*; Springer: Berlin/Heidelberg, Germany, 2017; pp. 143–169. [[CrossRef](#)]
15. Tang, X.; Zeng, X.; Li, Z.; Hu, L.; Sun, Y.; Liu, S.; Lei, T.; Lin, L. Production of  $\gamma$ -Valerolactone from Lignocellulosic Biomass for Sustainable Fuels and Chemicals Supply. *Renew. Sustain. Energy Rev.* **2014**, *40*, 608–620. [[CrossRef](#)]
16. Zhou, H.; Xu, H.; Wang, X.; Liu, Y. Convergent Production of 2,5-Furandicarboxylic Acid from Biomass and CO<sub>2</sub>. *Green Chem.* **2019**, *21*, 2923–2927. [[CrossRef](#)]
17. Verdini, F.; Gaudino, E.C.; Canova, E.; Tabasso, S.; Behbahani, P.J.; Cravotto, G. Lignin as a Natural Carrier for the Efficient Delivery of Bioactive Compounds: From Waste to Health. *Molecules* **2022**, *27*, 3598. [[CrossRef](#)]
18. Wang, S.; Dai, G.; Yang, H.; Luo, Z. Lignocellulosic Biomass Pyrolysis Mechanism: A State-of-the-Art Review. *Prog. Energy Combust. Sci.* **2017**, *62*, 33–86. [[CrossRef](#)]
19. Chai, L.; Hou, X.; Cui, X.; Li, H.; Zhang, N.; Zhang, H.; Chen, C.; Wang, Y.; Deng, T. 5-Hydroxymethylfurfural Oxidation to Maleic Acid by O<sub>2</sub> over Graphene Oxide Supported Vanadium: Solvent Effects and Reaction Mechanism. *Chem. Eng. J.* **2020**, *388*, 124187. [[CrossRef](#)]
20. Ahorsu, R.; Medina, F.; Constantí, M. Significance and Challenges of Biomass as a Suitable Feedstock for Bioenergy and Bio-chemical Production: A Review. *Energies* **2018**, *11*, 3366. [[CrossRef](#)]
21. Bellardita, M.; Loddo, V.; Palmisano, L. Formation of High Added Value Chemicals by Photocatalytic Treatment of Biomass. *Mini-Rev. Org. Chem.* **2020**, *17*, 884–901. [[CrossRef](#)]
22. Fonseca-Cervantes, O.R.; Pérez-Larios, A.; Romero Arellano, V.H.; Sulbaran-Rangel, B.; González, C.A.G. Effects in Band Gap for Photocatalysis in TiO<sub>2</sub> Support by Adding Gold and Ruthenium. *Processes* **2020**, *8*, 1032. [[CrossRef](#)]
23. Wu, X.; Chang, Y.; Lin, S. Titanium Radical Redox Catalysis: Recent Innovations in Catalysts, Reactions, and Modes of Activation. *Chem* **2022**, *8*, 1805–1821. [[CrossRef](#)]
24. Patnaik, S.; Sahoo, D.P.; Parida, K.M. Bimetallic Co-Effect of Au-Pd Alloyed Nanoparticles on Mesoporous Silica Modified g-C<sub>3</sub>N<sub>4</sub> for Single and Simultaneous Photocatalytic Oxidation of Phenol and Reduction of Hexavalent Chromium. *J. Colloid Interface Sci.* **2020**, *560*, 519–535. [[CrossRef](#)]
25. Chen, K.; Shen, T.; Lu, Y.; Hu, Y.; Wang, J.; Zhang, J.; Wang, D. Engineering Titanium Oxide-Based Support for Electrocatalysis. *J. Energy Chem.* **2022**, *67*, 168–183. [[CrossRef](#)]
26. Wu, X.; Li, J.; Xie, S.; Duan, P.; Zhang, H.; Feng, J.; Zhang, Q.; Cheng, J.; Wang, Y. Selectivity Control in Photocatalytic Valorization of Biomass-Derived Platform Compounds by Surface Engineering of Titanium Oxide. *Chem* **2020**, *6*, 3038–3053. [[CrossRef](#)]
27. Zhao, H.; Li, C.F.; Liu, L.Y.; Palma, B.; Hu, Z.Y.; Renneckar, S.; Larter, S.; Li, Y.; Kibria, M.G.; Hu, J.; et al. N-p Heterojunction of TiO<sub>2</sub>-NiO Core-Shell Structure for Efficient Hydrogen Generation and Lignin Photoreforming. *J. Colloid Interface Sci.* **2021**, *585*, 694–704. [[CrossRef](#)]
28. Segovia-Guzmán, M.O.; Román-Aguirre, M.; Verde-Gomez, J.Y.; Collins-Martínez, V.H.; Zaragoza-Galán, G.; Ramos-Sánchez, V.H. Green Cu<sub>2</sub>O/TiO<sub>2</sub> Heterojunction for Glycerol Photoreforming. *Catal. Today* **2020**, *349*, 88–97. [[CrossRef](#)]
29. Li, Y.; Yin, Q.; Zeng, Y.; Liu, Z. Hollow Spherical Biomass Derived-Carbon Dotted with SnS<sub>2</sub>/g-C<sub>3</sub>N<sub>4</sub> Z-Scheme Heterojunction for Efficient CO<sub>2</sub> Photoreduction into CO. *Chem. Eng. J.* **2022**, *438*, 135652. [[CrossRef](#)]
30. Yang, Q.; Wang, T.; Han, F.; Zheng, Z.; Xing, B.; Li, B. Bimetal-Modified g-C<sub>3</sub>N<sub>4</sub> Photocatalyst for Promoting Hydrogen Production Coupled with Selective Oxidation of Biomass Derivative. *J. Alloys Compd.* **2022**, *897*, 163177. [[CrossRef](#)]

31. Zhu, Y.; Zhang, Y.; Cheng, L.; Ismael, M.; Feng, Z.; Wu, Y. Novel Application of G-C<sub>3</sub>N<sub>4</sub>/NaNbO<sub>3</sub> Composite for Photocatalytic Selective Oxidation of Biomass-Derived HMF to FFCA under Visible Light Irradiation. *Adv. Powder Technol.* **2020**, *31*, 1148–1159. [[CrossRef](#)]
32. Zhang, H.; Feng, Z.; Zhu, Y.; Wu, Y.; Wu, T. Photocatalytic Selective Oxidation of Biomass-Derived 5-Hydroxymethylfurfural to 2,5-Diformylfuran on WO<sub>3</sub>/g-C<sub>3</sub>N<sub>4</sub> Composite under Irradiation of Visible Light. *J. Photochem. Photobiol. A Chem.* **2019**, *371*, 1–9. [[CrossRef](#)]
33. Patnaik, S.; Sahoo, D.P.; Parida, K. Recent Advances in Anion Doped G-C<sub>3</sub>N<sub>4</sub> Photocatalysts: A Review. *Carbon N. Y.* **2021**, *172*, 682–711. [[CrossRef](#)]
34. Cai, B.; Zhang, Y.; Feng, J.; Huang, C.; Ma, T.; Pan, H. Highly Efficient G-C<sub>3</sub>N<sub>4</sub> Supported Ruthenium Catalysts for the Catalytic Transfer Hydrogenation of Levulinic Acid to Liquid Fuel  $\gamma$ -Valerolactone. *Renew. Energy* **2021**, *177*, 652–662. [[CrossRef](#)]
35. Payormhorm, J.; Idem, R. Synthesis of C-Doped TiO<sub>2</sub> by Sol-Microwave Method for Photocatalytic Conversion of Glycerol to Value-Added Chemicals under Visible Light. *Appl. Catal. A Gen.* **2020**, *590*, 117362. [[CrossRef](#)]
36. Yoon, T.P.; Ischay, M.A.; Du, J. Visible Light Photocatalysis as a Greener Approach to Photochemical Synthesis. *Nat. Chem.* **2010**, *2*, 527–532. [[CrossRef](#)]
37. Wu, X.; Luo, N.; Xie, S.; Zhang, H.; Zhang, Q.; Wang, F.; Wang, Y. Photocatalytic Transformations of Lignocellulosic Biomass into Chemicals. *Chem. Soc. Rev.* **2020**, *49*, 6198–6223. [[CrossRef](#)]
38. Yan, K.; Li, H. State of the Art and Perspectives in Catalytic Conversion Mechanism of Biomass to Bio-aromatics. *Energy Fuels* **2021**, *35*, 45–62. [[CrossRef](#)]
39. Heng, Z.W.; Chong, W.C.; Pang, Y.L.; Koo, C.H. An Overview of the Recent Advances of Carbon Quantum Dots/Metal Oxides in the Application of Heterogeneous Photocatalysis in Photodegradation of Pollutants towards Visible-Light and Solar Energy Exploitation. *J. Environ. Chem. Eng.* **2021**, *9*, 105199. [[CrossRef](#)]
40. Lang, X.; Chen, X.; Zhao, J. Heterogeneous Visible Light Photocatalysis for Selective Organic Transformations. *Chem. Soc. Rev.* **2014**, *43*, 473–486. [[CrossRef](#)]
41. Yousuf, A.; Pirozzi, D.; Sannino, F. Fundamentals of Lignocellulosic Biomass. *Lignocellul. Biomass Liq. Biofuels* **2020**, 1–15. [[CrossRef](#)]
42. Colmenares, J.C.; Magdziarz, A. Room Temperature Versatile Conversion of Biomass-Derived Compounds by Means of Supported TiO<sub>2</sub> Photocatalysts. *J. Mol. Catal. A Chem.* **2013**, *366*, 156–162. [[CrossRef](#)]
43. Nguyen, J.D.; Matsuura, B.S.; Stephenson, C.R.J. A Photochemical Strategy for Lignin Degradation at Room Temperature. *J. Am. Chem. Soc.* **2014**, *136*, 1218–1221. [[CrossRef](#)]
44. Zhang, Y.; Naebe, M. Lignin: A Review on Structure, Properties, and Applications as a Light-Colored UV Absorber. *ACS Sustain. Chem. Eng.* **2021**, *9*, 1427–1442. [[CrossRef](#)]
45. Sannigrahi, P.; Pu, Y.; Ragauskas, A. Cellulosic Biorefineries-Unleashing Lignin Opportunities. *Curr. Opin. Environ. Sustain.* **2010**, *2*, 383–393. [[CrossRef](#)]
46. Xu, C.; Arancon, R.A.D.; Labidi, J.; Luque, R. Lignin Depolymerisation Strategies: Towards Valuable Chemicals and Fuels. *Chem. Soc. Rev.* **2014**, *43*, 7485–7500. [[CrossRef](#)]
47. Onokwai, A.O.; Ajisegiri, E.S.A.; Okokpujie, I.P.; Ibikunle, R.A.; Oki, M.; Dirisu, J.O. Characterization of Lignocellulose Biomass Based on Proximate, Ultimate, Structural Composition, and Thermal Analysis. *Mater. Today Proc.* **2022**, *65*, 2156–2162. [[CrossRef](#)]
48. Monir, M.U.; Abd Aziz, A.; Kristanti, R.A.; Yousuf, A. Gasification of Lignocellulosic Biomass to Produce Syngas in a 50 kW Downdraft Reactor. *Biomass Bioenerg.* **2018**, *119*, 335–345. [[CrossRef](#)]
49. Lee, C.S.; Conradi, A.V.; Lester, E. Review of Supercritical Water Gasification with Lignocellulosic Real Biomass as the Feedstocks: Process Parameters, Biomass Composition, Catalyst Development, Reactor Design and Its Challenges. *Chem. Eng. J.* **2021**, *415*, 128837. [[CrossRef](#)]
50. Cai, J.; Rahman, M.M.; Zhang, S.; Sarker, M.; Zhang, X.; Zhang, Y.; Yu, X.; Fini, E.H. Review on Aging of Bio-Oil from Biomass Pyrolysis and Strategy to Slowing Aging. *Energy Fuels* **2021**, *35*, 11665–11692. [[CrossRef](#)]
51. Blanco, E.; Sepulveda, C.; Cruces, K.; García-Fierro, J.L.; Ghampson, I.T.; Escalona, N. Conversion of Guaiacol over Metal Carbides Supported on Activated Carbon Catalysts. *Catal. Today* **2020**, *356*, 376–383. [[CrossRef](#)]
52. Kohli, K.; Prajapati, R.; Sharma, B.K. Bio-Based Chemicals from Renewable Biomass for Integrated Biorefineries. *Energies* **2019**, *12*, 233. [[CrossRef](#)]
53. Ma, B.; Wang, Y.; Guo, X.; Tong, X.; Liu, C.; Wang, Y.; Guo, X. Photocatalytic Synthesis of 2,5-Diformylfuran from 5-Hydroxymethylfurfural or Fructose over Bimetallic Au-Ru Nanoparticles Supported on Reduced Graphene Oxides. *Appl. Catal. A Gen.* **2018**, *552*, 70–76. [[CrossRef](#)]
54. Lozano, F.J.; Lozano, R. Assessing the Potential Sustainability Benefits of Agricultural Residues: Biomass Conversion to Syngas for Energy Generation or to Chemicals Production. *J. Clean. Prod.* **2018**, *172*, 4162–4169. [[CrossRef](#)]
55. Wang, M.; Ma, J.; Liu, H.; Luo, N.; Zhao, Z.; Wang, F. Sustainable Productions of Organic Acids and Their Derivatives from Biomass via Selective Oxidative Cleavage of C-C Bond. *ACS Catal.* **2018**, *8*, 2129–2165. [[CrossRef](#)]
56. Yoganandham, S.T.; Sathyamoorthy, G.; Renuka, R.R. Emerging Extraction Techniques: Hydrothermal Processing. *Seaweed Technol.* **2020**, 191–205. [[CrossRef](#)]
57. Li, X.; Shi, J.L.; Hao, H.; Lang, X. Visible Light-Induced Selective Oxidation of Alcohols with Air by Dye-Sensitized TiO<sub>2</sub> Photocatalysis. *Appl. Catal. B Environ.* **2018**, *232*, 260–267. [[CrossRef](#)]

58. Marci, G.; García-López, E.I.; Palmisano, L. Polymeric Carbon Nitride (C<sub>3</sub>N<sub>4</sub>) as Heterogeneous Photocatalyst for Selective Oxidation of Alcohols to Aldehydes. *Catal. Today* **2018**, *315*, 126–137. [[CrossRef](#)]
59. Chen, L.; Tang, J.; Song, L.N.; Chen, P.; He, J.; Au, C.T.; Yin, S.F. Heterogeneous Photocatalysis for Selective Oxidation of Alcohols and Hydrocarbons. *Appl. Catal. B Environ.* **2019**, *242*, 379–388. [[CrossRef](#)]
60. Wan, Y.; Zhang, L.; Chen, Y.; Lin, J.; Hu, W.; Wang, S.; Lin, J.; Wan, S.; Wang, Y. One-Pot Synthesis of Gluconic Acid from Biomass-Derived Levoglucosan Using a Au/Cs<sub>2</sub>H<sub>0.5</sub>PW<sub>12</sub>O<sub>40</sub> Catalyst. *Green Chem.* **2019**, *21*, 6318–6325. [[CrossRef](#)]
61. Fung, C.M.; Tang, J.Y.; Tan, L.L.; Mohamed, A.R.; Chai, S.P. Recent Progress in Two-Dimensional Nanomaterials for Photocatalytic Carbon Dioxide Transformation into Solar Fuels. *Mater. Today Sustain.* **2020**, *9*, 100037. [[CrossRef](#)]
62. Du, C.; Wang, X.; Chen, W.; Feng, S.; Wen, J.; Wu, Y.A. CO<sub>2</sub> Transformation to Multicarbon Products by Photocatalysis and Electrocatalysis. *Mater. Today Adv.* **2020**, *6*, 100071. [[CrossRef](#)]
63. Wang, Q.; Domen, K. Particulate Photocatalysts for Light-Driven Water Splitting: Mechanisms, Challenges, and Design Strategies. *Chem. Rev.* **2020**, *120*, 919–985. [[CrossRef](#)]
64. Ibhaddon, A.O.; Fitzpatrick, P. Heterogeneous Photocatalysis: Recent Advances and Applications. *Catalysts* **2013**, *3*, 189–218. [[CrossRef](#)]
65. Akerdi, A.G.; Bahrami, S.H. Application of Heterogeneous Nano-Semiconductors for Photocatalytic Advanced Oxidation of Organic Compounds: A Review. *J. Environ. Chem. Eng.* **2019**, *7*, 103283. [[CrossRef](#)]
66. Augugliaro, V.; Camera-Roda, G.; Loddo, V.; Palmisano, G.; Palmisano, L.; Soria, J.; Yurdakal, S. Heterogeneous Photo-catalysis and Photoelectrocatalysis: From Unselective Abatement of Noxious Species to Selective Production of High-Value Chemicals. *J. Phys. Chem. Lett.* **2015**, *6*, 1968–1981. [[CrossRef](#)]
67. Li, Z.; Meng, X. New Insight into Reactive Oxidation Species (ROS) for Bismuth-Based Photocatalysis in Phenol Removal. *J. Hazard. Mater.* **2020**, *399*, 122939. [[CrossRef](#)]
68. Zhu, Y.; Li, Z.; Chen, J. Applications of Lignin-Derived Catalysts for Green Synthesis. *Green Energy Environ.* **2019**, *4*, 210–244. [[CrossRef](#)]
69. Chen, Z.; Wang, J.; Xing, R.; Wang, Y.; Wang, S.; Wei, D.; Li, J.; Chen, Z.; Lü, J. Preparation of Carbon-Supported CdS Photocatalysts with High Performance of Dye Photodegradation Using Cadmium-Enriched Perilla Frutescens Biomass. *Inorg. Chem. Commun.* **2019**, *109*, 107559. [[CrossRef](#)]
70. Liu, X.Q.; Chen, W.J.; Jiang, H. Facile Synthesis of Ag/Ag<sub>3</sub>PO<sub>4</sub>/AMB Composite with Improved Photocatalytic Performance. *Chem. Eng. J.* **2017**, *308*, 889–896. [[CrossRef](#)]
71. Ren, Z.; Chen, F.; Wen, K.; Lu, J. Enhanced Photocatalytic Activity for Tetracyclines Degradation with Ag Modified G-C<sub>3</sub>N<sub>4</sub> Composite under Visible Light. *J. Photochem. Photobiol. A Chem.* **2020**, *389*, 112217. [[CrossRef](#)]
72. Zhao, R.; Sun, X.; Jin, Y.; Han, J.; Wang, L.; Liu, F. Au/Pd/g-C<sub>3</sub>N<sub>4</sub> Nanocomposites for Photocatalytic Degradation of Tetracycline Hydrochloride. *J. Mater. Sci.* **2019**, *54*, 5445–5456. [[CrossRef](#)]
73. Asencios, Y.J.O.; Lourenço, V.S.; Carvalho, W.A. Removal of Phenol in Seawater by Heterogeneous Photocatalysis Using Activated Carbon Materials Modified with TiO<sub>2</sub>. *Catal. Today* **2022**, *388–389*, 247–258. [[CrossRef](#)]
74. Khan, A.A.; Tahir, M. Recent Advancements in Engineering Approach towards Design of Photo-Reactors for Selective Photocatalytic CO<sub>2</sub> Reduction to Renewable Fuels. *J. CO<sub>2</sub> Util.* **2019**, *29*, 205–239. [[CrossRef](#)]
75. Kuriki, R.; Yamamoto, M.; Higuchi, K.; Yamamoto, Y.; Akatsuka, M.; Lu, D.; Yagi, S.; Yoshida, T.; Ishitani, O.; Maeda, K. Robust Binding between Carbon Nitride Nanosheets and a Binuclear Ruthenium(II) Complex Enabling Durable, Selective CO<sub>2</sub> Reduction under Visible Light in Aqueous Solution. *Angew. Chemie Int. Ed.* **2017**, *56*, 4867–4871. [[CrossRef](#)]
76. Ahmed, N.; Morikawa, M.; Izumi, Y. Photocatalytic Conversion of Carbon Dioxide into Methanol Using Optimized Layered Double Hydroxide Catalysts. *Catal. Today* **2012**, *185*, 263–269. [[CrossRef](#)]
77. Tasbihi, M.; Schwarze, M.; Edelmánová, M.; Spöri, C.; Strasser, P.; Schomäcker, R. Photocatalytic Reduction of CO<sub>2</sub> to Hydrocarbons by Using Photodeposited Pt Nanoparticles on Carbon-Doped Titania. *Catal. Today* **2019**, *328*, 8–14. [[CrossRef](#)]
78. Meng, S.; Ye, X.; Zhang, J.; Fu, X.; Chen, S. Effective Use of Photogenerated Electrons and Holes in a System: Photocatalytic Selective Oxidation of Aromatic Alcohols to Aldehydes and Hydrogen Production. *J. Catal.* **2018**, *367*, 159–170. [[CrossRef](#)]
79. López-Tenllado, F.J.; Marinas, A.; Urbano, F.J.; Colmenares, J.C.; Hidalgo, M.C.; Marinas, J.M.; Moreno, J.M. Selective Photooxidation of Alcohols as Test Reaction for Photocatalytic Activity. *Appl. Catal. B Environ.* **2012**, *128*, 150–158. [[CrossRef](#)]
80. Yuan, B.; Zhang, B.; Wang, Z.; Lu, S.; Li, J.; Liu, Y.; Li, C. Photocatalytic Aerobic Oxidation of Toluene and Its Derivatives to Aldehydes on Pd/Bi<sub>2</sub>WO<sub>6</sub>. *Chin. J. Catal.* **2017**, *38*, 440–446. [[CrossRef](#)]
81. Thakur, S.; Kaur, K.; Das, N.; Pal, B. Photo-Oxidation Kinetics of Sugars Having Different Molecular Size and Glycosidic Linkages for Their Complete Mineralization to Subunits by Bare/Ag–TiO<sub>2</sub> under U.V. Irradiation. *J. Taiwan Inst. Chem. Eng.* **2017**, *80*, 488–494. [[CrossRef](#)]
82. Albert, J. Selective Oxidation of Lignocellulosic Biomass to Formic Acid and High-Grade Cellulose Using Tailor-Made Polyoxometalate Catalysts. *Faraday Discuss.* **2017**, *202*, 99–109. [[CrossRef](#)]
83. Li, X.; Chen, Y.; Tao, Y.; Shen, L.; Xu, Z.; Bian, Z.; Li, H. Challenges of Photocatalysis and Their Coping Strategies. *Chem. Catal.* **2022**, *2*, 1315–1345. [[CrossRef](#)]
84. Jin, C.; Dai, Y.; Wei, W.; Ma, X.; Li, M.; Huang, B. Effects of Single Metal Atom (Pt, Pd, Rh and Ru) Adsorption on the Photocatalytic Properties of Anatase TiO<sub>2</sub>. *Appl. Surf. Sci.* **2017**, *426*, 639–646. [[CrossRef](#)]

85. Wakerley, D.W.; Kuehnel, M.F.; Orchard, K.L.; Ly, K.H.; Rosser, T.E.; Reisner, E. Solar-Driven Re-forming of Lignocellulose to H<sub>2</sub> with a CdS/CdOx Photocatalyst. *Nat. Energy* **2017**, *24*, 17021. [[CrossRef](#)]
86. Zhao, H.; Li, C.F.; Yu, X.; Zhong, N.; Hu, Z.Y.; Li, Y.; Larter, S.; Kibria, M.G.; Hu, J. Mechanistic Understanding of Cellulose  $\beta$ -1,4-Glycosidic Cleavage via Photocatalysis. *Appl. Catal. B Environ.* **2022**, *302*, 120872. [[CrossRef](#)]
87. Speltini, A.; Sturini, M.; Dondi, D.; Annovazzi, E.; Maraschi, F.; Caratto, V.; Profumo, A.; Buttafava, A. Sunlight-Promoted Photocatalytic Hydrogen Gas Evolution from Water-Suspended Cellulose: A Systematic Study. *Photochem. Photobiol. Sci.* **2014**, *13*, 1410–1419. [[CrossRef](#)]
88. Han, G.; Jin, Y.H.; Burgess, R.A.; Dickenson, N.E.; Cao, X.M.; Sun, Y. Visible-Light-Driven Valorization of Biomass Intermediates Integrated with H<sub>2</sub> Production Catalyzed by Ultrathin Ni/CdS Nanosheets. *J. Am. Chem. Soc.* **2017**, *139*, 15584–15587. [[CrossRef](#)]
89. Low, J.; Yu, J.; Jaroniec, M.; Wageh, S.; Al-Ghamdi, A.A. Heterojunction Photocatalysts. *Adv. Mater.* **2017**, *29*, 1601694. [[CrossRef](#)]
90. Wu, X.; Liu, C.; Li, X.; Zhang, X.; Wang, C.; Liu, Y. Effect of Morphology on the Photocatalytic Activity of G-C<sub>3</sub>N<sub>4</sub> Photocatalysts under Visible-Light Irradiation. *Mater. Sci. Semicond. Process.* **2015**, *32*, 76–81. [[CrossRef](#)]
91. Gong, J.; Imbault, A.; Farnood, R. The Promoting Role of Bismuth for the Enhanced Photocatalytic Oxidation of Lignin on Pt-TiO<sub>2</sub> under Solar Light Illumination. *Appl. Catal. B Environ.* **2017**, *204*, 296–303. [[CrossRef](#)]
92. Jongprateep, O.; Meesombad, K.; Techapiesanchaenokij, R.; Surawathanawises, K. Chemical Composition, Microstructure, Bandgap Energy and Electrochemical Activities of TiO<sub>2</sub> and Ag-Doped TiO<sub>2</sub> Powder Synthesized by Solution Combustion Technique. *Ceram. Int.* **2018**, *44*, S228–S232. [[CrossRef](#)]
93. Marci, G.; García-López, E.I.; Pomilla, F.R.; Palmisano, L.; Zaffora, A.; Santamaria, M.; Krivtsov, I.; Ilkaeva, M.; Barbieriková, Z.; Brezová, V. Photoelectrochemical and EPR Features of Polymeric C<sub>3</sub>N<sub>4</sub> and O-Modified C<sub>3</sub>N<sub>4</sub> Employed for Selective Photocatalytic Oxidation of Alcohols to Aldehydes. *Catal. Today* **2019**, *328*, 21–28. [[CrossRef](#)]
94. Shiamala, L.; Alamelu, K.; Raja, V.; Jaffar Ali, B.M. Synthesis, Characterization and Application of TiO<sub>2</sub>–Bi<sub>2</sub>WO<sub>6</sub> Nanocomposite Photocatalyst for Pretreatment of Starch Biomass and Generation of Biofuel Precursors. *J. Environ. Chem. Eng.* **2018**, *6*, 3306–3321. [[CrossRef](#)]
95. Zhang, Y.; Li, Q.; Gao, Q.; Wan, S.; Yao, P.; Zhu, X. Preparation of Ag/ $\beta$ -Cyclodextrin Co-Doped TiO<sub>2</sub> Floating Photocatalytic Membrane for Dynamic Adsorption and Photoactivity under Visible Light. *Appl. Catal. B Environ.* **2020**, *267*, 118715. [[CrossRef](#)]
96. Wang, Y.; Lai, Q.; He, Y.; Fan, M. Selective Photocatalytic Carbon Dioxide Conversion with Pt@Ag-TiO<sub>2</sub> Nanoparticles. *Catal. Commun.* **2018**, *108*, 98–102. [[CrossRef](#)]
97. Preethi, L.K.; Mathews, T.; Nand, M.; Jha, S.N.; Gopinath, C.S.; Dash, S. Band Alignment and Charge Transfer Pathway in Three Phase Anatase-Rutile-Brookite TiO<sub>2</sub> Nanotubes: An Efficient Photocatalyst for Water Splitting. *Appl. Catal. B Environ.* **2017**, *218*, 9–19. [[CrossRef](#)]
98. Liu, X.; Dong, G.; Li, S.; Lu, G.; Bi, Y. Direct Observation of Charge Separation on Anatase TiO<sub>2</sub> Crystals with Selectively Etched {001} Facets. *J. Am. Chem. Soc.* **2016**, *138*, 2917–2920. [[CrossRef](#)]
99. Zhang, D.; Dong, S. Challenges in Band Alignment between Semiconducting Materials: A Case of Ru-tilde and Anatase TiO<sub>2</sub>. *Prog. Nat. Sci. Mater. Int.* **2019**, *29*, 277–284. [[CrossRef](#)]
100. Zhang, Y.F.; Lin, W.; Li, Y.; Ding, K.N.; Li, J.Q. A Theoretical Study on the Electronic Structures of TiO<sub>2</sub>: Effect of Hartree–Fock Exchange. *J. Phys. Chem. B* **2005**, *109*, 19270–19277. [[CrossRef](#)]
101. Momma, K.; Izumi, F. VESTA 3 for Three-Dimensional Visualization of Crystal, Volumetric and Morphology Data. *J. Appl. Crystallogr.* **2011**, *44*, 1272–1276. [[CrossRef](#)]
102. Downs, R.; Hall-Wallace, M. American Mineralogist Crystal Structure Database. *Am. Mineral.* **2003**, *88*, 247–250.
103. Kavan, L.; Grätzel, M.; Gilbert, S.E.; Klemenz, C.; Scheel, H.J. Electrochemical and Photoelectrochemical Investigation of Single-Crystal Anatase. *J. Am. Chem. Soc.* **1996**, *118*, 6716–6723. [[CrossRef](#)]
104. Zhang, X.; Lin, Y.; He, D.; Zhang, J.; Fan, Z.; Xie, T. Interface Junction at Anatase/Rutile in Mixed-Phase TiO<sub>2</sub>: Formation and Photo-Generated Charge Carriers Properties. *Chem. Phys. Lett.* **2011**, *504*, 71–75. [[CrossRef](#)]
105. Xiong, G.; Shao, R.; Droubay, T.C.; Joly, A.G.; Beck, K.M.; Chambers, S.A.; Hess, W.P. Photoemission Electron Microscopy of TiO<sub>2</sub> Anatase Films Embedded with Rutile Nanocrystals. *Adv. Funct. Mater.* **2007**, *17*, 2133–2138. [[CrossRef](#)]
106. Scanlon, D.O.; Dunnill, C.W.; Buckeridge, J.; Shevlin, S.A.; Logsdail, A.J.; Woodley, S.M.; Catlow, C.R.A.; Powell, M.J.; Palgrave, R.G.; Parkin, I.P.; et al. Band Alignment of Rutile and Anatase TiO<sub>2</sub>. *Nat. Mater.* **2013**, *12*, 798–801. [[CrossRef](#)]
107. Ilkaeva, M.; Krivtsov, I.; García, J.R.; Díaz, E.; Ordóñez, S.; García-López, E.I.; Marci, G.; Palmisano, L.; Maldonado, M.I.; Malato, S. Selective Photocatalytic Oxidation of 5-Hydroxymethyl-2-Furfural in Aqueous Suspension of Polymeric Carbon Nitride and Its Adduct with H<sub>2</sub>O<sub>2</sub> in a Solar Pilot Plant. *Catal. Today* **2018**, *315*, 138–148. [[CrossRef](#)]
108. Wang, J.; Wang, S. A Critical Review on Graphitic Carbon Nitride (g-C<sub>3</sub>N<sub>4</sub>)-Based Materials: Preparation, Modification and Environmental Application. *Coord. Chem. Rev.* **2022**, *453*, 214338. [[CrossRef](#)]
109. Kavitha, R.; Nithya, P.M.; Girish Kumar, S. Noble Metal Deposited Graphitic Carbon Nitride Based Heterojunction Photocatalysts. *Appl. Surf. Sci.* **2020**, *508*, 145142. [[CrossRef](#)]
110. Yan, D.; Wu, X.; Pei, J.; Wu, C.; Wang, X.; Zhao, H. Construction of G-C<sub>3</sub>N<sub>4</sub>/TiO<sub>2</sub>/Ag Composites with Enhanced Visible-Light Photocatalytic Activity and Antibacterial Properties. *Ceram. Int.* **2020**, *46*, 696–702. [[CrossRef](#)]
111. Ma, J.; Yu, X.; Liu, X.; Li, H.; Hao, X.; Li, J. The Preparation and Photocatalytic Activity of Ag-Pd/g-C<sub>3</sub>N<sub>4</sub> for the Coupling Reaction between Benzyl Alcohol and Aniline. *Mol. Catal.* **2019**, *476*, 110533. [[CrossRef](#)]

112. Liang, H.; Wang, J.; Jin, B.; Li, D.; Men, Y. Direct Growth of Au Nanoparticles on g-C<sub>3</sub>N<sub>4</sub> for Photo-catalytic Selective Alcohol Oxidations. *Inorg. Chem. Commun.* **2019**, *109*, 107574. [[CrossRef](#)]
113. Nair, V.; Dhar, P.; Vinu, R. Production of Phenolics via Photocatalysis of Ball Milled Lignin–TiO<sub>2</sub> Mixtures in Aqueous Suspension. *RSC Adv.* **2016**, *6*, 18204–18216. [[CrossRef](#)]
114. Darabdhara, G.; Das, M.R. Bimetallic Au-Pd Nanoparticles on 2D Supported Graphitic Carbon Nitride and Reduced Graphene Oxide Sheets: A Comparative Photocatalytic Degradation Study of Organic Pollutants in Water. *Chemosphere* **2018**, *197*, 817–829. [[CrossRef](#)]
115. Grabowska, E.; Marchelek, M.; Klimczuk, T.; Lisowski, W.; Zaleska-Medynska, A. Preparation, Characterization and Photocatalytic Activity of TiO<sub>2</sub> Microspheres Decorated by Bimetallic Nanoparticles. *J. Mol. Catal. A Chem.* **2016**, *424*, 241–253. [[CrossRef](#)]
116. Cybula, A.; Priebe, J.B.; Pohl, M.M.; Sobczak, J.W.; Schneider, M.; Zielińska-Jurek, A.; Brückner, A.; Zaleska, A. The Effect of Calcination Temperature on Structure and Photocatalytic Properties of Au/Pd Nanoparticles Supported on TiO<sub>2</sub>. *Appl. Catal. B Environ.* **2014**, *152–153*, 202–211. [[CrossRef](#)]
117. Nguyen, T.T.H.; Le, M.C.; Ha, N.N. Understanding the Influence of Single Metal (Li, Mg, Al, Fe, Ag) Doping on the Electronic and Optical Properties of g-C<sub>3</sub>N<sub>4</sub>: A Theoretical Study. *Mol. Simul.* **2020**, *47*, 10–17. [[CrossRef](#)]
118. Yang, C.; Zhang, G.; Meng, Y.; Pan, G.; Ni, Z.; Xia, S. Direct Z-Scheme CeO<sub>2</sub>@LDH Core–Shell Heterostructure for Photodegradation of Rhodamine B by Synergistic Persulfate Activation. *J. Hazard. Mater.* **2021**, *408*, 124908. [[CrossRef](#)]
119. Raizada, P.; Kumar, A.; Hasiya, V.; Singh, P.; Thakur, V.K.; Khan, A.A.P. An Overview of Converting Reductive Photocatalyst into All Solid-State and Direct Z-Scheme System for Water Splitting and CO<sub>2</sub> Reduction. *J. Ind. Eng. Chem.* **2021**, *93*, 1–27. [[CrossRef](#)]
120. Shao, Y.R.; Zhou, L.; Yu, L.; Li, Z.F.; Li, Y.T.; Li, W.; Hu, T.L. In Situ Construction of a Co/ZnO@C Heterojunction Catalyst for Efficient Hydrogenation of Biomass Derivative under Mild Conditions. *ACS Appl. Mater. Interfaces* **2022**, *14*, 17195–17207. [[CrossRef](#)]
121. Chen, S.; Qian, T.T.; Ling, L.L.; Zhang, W.; Gong, B.B.; Jiang, H. Hydrogenation of Furfural to Cyclopentanone under Mild Conditions by a Structure-Optimized Ni–NiO/TiO<sub>2</sub> Heterojunction Catalyst. *ChemSusChem* **2020**, *13*, 5507–5515. [[CrossRef](#)]
122. Dutta, S.; Bhat, N.S. Catalytic Transformation of Biomass-Derived Furfurals to Cyclopentanones and Their Derivatives: A Review. *ACS Omega* **2021**, *6*, 35145–35172. [[CrossRef](#)]
123. Fernández, M.A.; Silva, O.F.; Vico, R.V.; de Rossi, R.H. Complex Systems That Incorporate Cyclodextrins to Get Materials for Some Specific Applications. *Carbohydr. Res.* **2019**, *480*, 12–34. [[CrossRef](#)]
124. Espinoza-Villalobos, N.; Rojas, S.; Salazar, R.A.; Contreras, D.; Escalona, N.; Vergara, E.; Laguna-Bercero, M.A.; Mendizabal, F.; Barrientos, L. Role of β-CD Macromolecule Anchored to α-Fe<sub>2</sub>O<sub>3</sub>/TiO<sub>2</sub> on the Selectivity and Partial Oxidation of Guaiacol to Add-Value Products. *ACS Sustain. Chem. Eng.* **2021**, *9*, 11427–11438. [[CrossRef](#)]
125. Lannoy, A.; Kania, N.; Bleta, R.; Fourmentin, S.; Machut-Binkowski, C.; Monflier, E.; Ponchel, A. Photocatalysis of Volatile Organic Compounds in Water: Towards a Deeper Understanding of the Role of Cyclodextrins in the Photodegradation of Toluene over Titanium Dioxide. *J. Colloid Interface Sci.* **2016**, *461*, 317–325. [[CrossRef](#)]
126. Liu, Q.; Zhou, Y.; Lu, J.; Zhou, Y. Novel Cyclodextrin-Based Adsorbents for Removing Pollutants from Wastewater: A Critical Review. *Chemosphere* **2020**, *241*, 125043. [[CrossRef](#)]
127. Crumling, M.A.; King, K.A.; Duncan, R.K. Cyclodextrins and Iatrogenic Hearing Loss: New Drugs with Significant Risk. *Front. Cell. Neurosci.* **2017**, *11*, 355. [[CrossRef](#)]
128. Chen, X.; Liu, D.; Wu, Z.; Cravotto, G.; Wu, Z.; Ye, B.C. Microwave-Assisted Rapid Synthesis of Ag-β-Cyclodextrin/TiO<sub>2</sub>/A.C. with Exposed {001} Facets for Highly Efficient Naphthalene Degradation under Visible Light. *Catal. Commun.* **2018**, *104*, 96–100. [[CrossRef](#)]
129. Yasuda, M.; Miura, A.; Yuki, R.; Nakamura, Y.; Shiragami, T.; Ishii, Y.; Yokoi, H. The Effect of TiO<sub>2</sub>-Photocatalytic Pretreatment on the Biological Production of Ethanol from Lignocelluloses. *J. Photochem. Photobiol. A Chem.* **2011**, *220*, 195–199. [[CrossRef](#)]
130. Zhang, G.; Ni, C.; Huang, X.; Welgamage, A.; Lawton, L.A.; Robertson, P.K.J.; Irvine, J.T.S. Simultaneous Cellulose Conversion and Hydrogen Production Assisted by Cellulose Decomposition under UV-Light Photocatalysis. *Chem. Commun.* **2016**, *52*, 1673–1676. [[CrossRef](#)]
131. Yin, J.; Zhang, Q.; Yang, C.; Zhang, B.; Deng, K. Highly Selective Oxidation of Glucose to Gluconic Acid and Glucaric Acid in Water Catalyzed by an Efficient Synergistic Photocatalytic System. *Catal. Sci. Technol.* **2020**, *10*, 2231–2241. [[CrossRef](#)]
132. Jin, B.; Yao, G.; Wang, X.; Ding, K.; Jin, F. Photocatalytic Oxidation of Glucose into Formate on Nano TiO<sub>2</sub> Catalyst. *ACS Sustain. Chem. Eng.* **2017**, *5*, 6377–6381. [[CrossRef](#)]
133. Chong, R.; Li, J.; Ma, Y.; Zhang, B.; Han, H.; Li, C. Selective Conversion of Aqueous Glucose to Value-Added Sugar Aldose on TiO<sub>2</sub>-Based Photocatalysts. *J. Catal.* **2014**, *314*, 101–108. [[CrossRef](#)]
134. Navakoteswara Rao, V.; Malu, T.J.; Cheralathan, K.K.; Sakar, M.; Pitchaimuthu, S.; Rodríguez-González, V.; Mamatha Kumari, M.; Shankar, M.V. Light-Driven Transformation of Biomass into Chemicals Using Photo-catalysts—Vistas and Challenges. *J. Environ. Manag.* **2021**, *284*, 111983–111994. [[CrossRef](#)]
135. Bellardita, M.; García-López, E.I.; Marci, G.; Palmisano, L. Photocatalytic Formation of H<sub>2</sub> and Value-Added Chemicals in Aqueous Glucose (Pt)-TiO<sub>2</sub> Suspension. *Int. J. Hydrogen Energy* **2016**, *41*, 5934–5947. [[CrossRef](#)]
136. Wang, L.; Zhang, Z.; Zhang, L.; Xue, S.; Doherty, W.O.S.; O'Hara, I.M.; Ke, X. Sustainable Conversion of Cellulosic Biomass to Chemicals under Visible-Light Irradiation. *RSC Adv.* **2015**, *5*, 85242–85247. [[CrossRef](#)]

137. Zou, J.; Zhang, G.; Xu, X. One-Pot Photoreforming of Cellulosic Biomass Waste to Hydrogen by Merging Photocatalysis with Acid Hydrolysis. *Appl. Catal. A Gen.* **2018**, *563*, 73–79. [[CrossRef](#)]
138. Kim, S.; Chmely, S.C.; Nimlos, M.R.; Bomble, Y.J.; Foust, T.D.; Paton, R.S.; Beckham, G.T. Computational Study of Bond Dissociation Enthalpies for a Large Range of Native and Modified Lignins. *J. Phys. Chem. Lett.* **2011**, *2*, 2846–2852. [[CrossRef](#)]
139. Gazi, S.; Hung Ng, W.K.; Ganguly, R.; Putra Moeljadi, A.M.; Hirao, H.; Soo, H. Selective Photocatalytic C-C Bond Cleavage under Ambient Conditions with Earth Abundant Vanadium Complexes. *Chem. Sci.* **2015**, *6*, 7130–7142. [[CrossRef](#)]
140. Kamwilaisak, K.; Wright, P.C. Investigating Laccase and Titanium Dioxide for Lignin Degradation. *Energy Fuels* **2012**, *26*, 2400–2406. [[CrossRef](#)]
141. Kärkä, M.D.; Bosque, I.; Matsuura, B.S.; Stephenson, C.R.J. Photocatalytic Oxidation of Lignin Model Systems by Merging Visible-Light Photoredox and Palladium Catalysis. *Org. Lett.* **2016**, *18*, 5166–5169. [[CrossRef](#)]
142. Ahmad, K.; Roy Ghatak, H.; Ahuja, S.M. Kinetics of Producing Vanillin and 4-Hydroxy Benzaldehyde from the Hydrolysis Residue of Rice Straw by Photocatalysis. *React. Kinet. Mech. Catal.* **2020**, *131*, 383–395. [[CrossRef](#)]
143. Srisasiwimon, N.; Chuangchote, S.; Laosiripojana, N.; Sagawa, T. TiO<sub>2</sub>/Lignin-Based Carbon Compositing Photocatalysts for Enhanced Photocatalytic Conversion of Lignin to High-Value Chemicals. *ACS Sustain. Chem. Eng.* **2018**, *6*, 13968–13976. [[CrossRef](#)]
144. Tian, M.; Wen, J.; MacDonald, D.; Asmussen, R.M.; Chen, A. A Novel Approach for Lignin Modification and Degradation. *Electrochem. Commun.* **2010**, *12*, 527–530. [[CrossRef](#)]